İSTANBUL TECHNICAL UNIVERSITY ★ INSTITUTE OF SCIENCE AND TECHNOLOGY

DYNAMIC NONLINEAR BEHAVIOR OF COMPOSITE PLATES

Ph.D. Thesis by

Hakan TANRIÖVER, M.Sc.

Department : **Mechanical Engineering**

Programme: **Construction and Manufacturing**

NOVEMBER 2005

İSTANBUL TECHNICAL UNIVERSITY ★ INSTITUTE OF SCIENCE AND TECHNOLOGY

DYNAMIC NONLINEAR BEHAVIOR OF COMPOSITE PLATES

Ph.D. Thesis by

Hakan TANRIÖVER, M.Sc.

(503002200)

Date of submission : 16 June 2005

Date of defence examination: 8 November 2005

Supervisor (Chairman): Assoc. Prof. Dr. Erol ŞENOCAK

Members of the Examining Committee Prof.Dr. M. Cengiz DÖKMECİ (İ.T.U.)

Prof.Dr. Alaeddin ARPACI (İ.T.U.)

Prof.Dr. Günay ANLAŞ (B.U.)

Prof.Dr. Uğur GÜVEN (Y.T.U.)

NOVEMBER 2005

İSTANBUL TEKNİK ÜNİVERSİTESİ ★ FEN BİLİMLERİ ENSTİTÜSÜ

KOMPOZİT PLAKLARIN DİNAMİK NONLİNEER DAVRANIŞI

DOKTORA TEZİ
Y. Müh. Hakan TANRIÖVER
(503002200)

Tezin Enstitüye Verildiği Tarih : 16 Haziran 2005
Tezin Savunulduğu Tarih : 8 Kasım 2005

Tez Danışmanı :	Doç.Dr. Erol ŞENOCAK
Diğer Jüri Üyeleri	Prof.Dr. M. Cengiz DÖKMECİ (İ.T.Ü.)
	Prof.Dr. Alaeddin ARPACI (İ.T.Ü.)
	Prof.Dr. Günay ANLAŞ (B.Ü.)
	Prof.Dr. Uğur GÜVEN (Y.T.Ü.)

KASIM 2005

ACKNOWLEDGEMENTS

I would like to thank to my supervisor Assoc. Prof. Dr. Erol Şenocak for his valuable help, patience and understanding in the course of this thesis work. My friend and colleague H. Gökmen Aksoy is valuable to me for his never-ending support. I would like to give special thanks to my family to whom this thesis work is dedicated.

November 2005 Hakan TANRIÖVER, M.Sc.

CONTENTS

ABBREVIATIONS v
LIST OF TABLES vi
LIST OF FIGURES vii
LIST OF SYMBOLS viii
SUMMARY ix
ÖZET x

1. INTRODUCTION 1
1.1 Description of the Problem 1
1.2 Definitions 2
1.2.1 Composite laminate 2
1.2.2 Types of loading in dynamic analysis 2
1.3 Literature Review 4
1.4 Objectives and Scope of the Thesis Work 7
1.5 Outline of the Thesis 8

2. GEOMETRIC NONLINEARITY FOR PLATES 9
2.1 Displacements and Strains in a Three-Dimensional Body 9
2.2 Geometric Nonlinearity 11
2.2.1 Large deflection of a plate 13

3. AN OVERVIEW OF LAMINATED PLATE THEORIES 15
3.1 Single Layer Theories 16
3.1.1 Classical laminated plate theory 16
3.1.2 First order shear deformation theory 17
3.1.3 Higher order theories 18
3.2 Layerwise Theories 19

4. GEOMETRICALLY NONLINEAR BEHAVIOR OF MODERATELY THICK LAMINATED COMPOSITE PLATES 22
4.1 Governing Equations 22
4.2 Solution Procedure 30
4.3 Boundary Conditions 32

5. LARGE DEFLECTION ANALYSIS OF MODERATELY THICK LAMINATED COMPOSITE PLATES 33
5.1 Numerical Examples 33
5.1.1 Symmetric cross-ply laminate 33
5.1.2 Unsymmetric laminates 35

6. NONLINEAR TRANSIENT ANALYSIS **38**
6.1 Time Integration 38
6.2 Numerical Examples 39
6.2.1 Linear transient analysis 40
6.2.2 Nonlinear transient analysis of an unsymmetric cross-ply laminate 40
6.2.3 Nonlinear transient analysis of an unsymmetric angle-ply laminate 41

7. CONCLUSIONS AND FUTURE WORK **43**

REFERENCES **44**

VITA **50**

ABBREVIATIONS

CLPT : Classical Laminated Plate Theory
CP : Chebyshev Polinomials
CS : Chebyshev Series
ESLTs : Equivalent Single Layer Theories
FEM : Finite Element Method
FSDT : First Order Shear Deformation Theory
GM : Galerkin Method
LWTs : Layerwise Theories

LIST OF TABLES

			Page
Table 4.1	**:**	Boundary conditions and corresponding weight functions.....	32
Table 5.1	**:**	Normalized center deflection (w') of the plate under SS–1 boundary condition.....	34
Table 5.2	**:**	Normalized center deflection (w') of the plate under CC–1 boundary condition.....	35

LIST OF FIGURES

			Page
Figure 1.1	:	*n*-layered composite laminate.....	2
Figure 1.2	:	a) Harmonic. b) Periodic. c) Transient. d) Stationary random. e) Non-stationary random.....	3
Figure 2.1	:	Deformation of a three-dimensional solid body.....	10
Figure 2.2	:	Configuration of a line element before and after deformation...	11
Figure 2.3	:	A plate with a coordinate system and dimensions.....	13
Figure 3.1	:	a) Classical laminated plate theory. b) First order shear deformation theory.....	16
Figure 4.1	:	Plate geometry and loading.....	22
Figure 5.1	:	Load (q') versus central deflection (w') of $[0^0/90^0/90^0/0^0]$ laminate.....	34
Figure 5.2	:	Load (q') versus M'_x (a) and M'_y (b) at the center of $[0^0/90^0/90^0/0^0]$ laminate.....	34
Figure 5.3	:	Load (q') versus central deflection (w') of cross-ply $[0^0/90^0]$ (CRS) and angle-ply $[45^0/\text{-}45^0]$ (ANG) laminates.....	36
Figure 5.4	:	Load q' versus center stress $\sigma'_x = \sigma_x\big\|_{\bar{x}=\bar{y}=0}(a/h)^2/E_2$ for cross-ply $[0^0/90^0]$ (CRS) laminate.....	36
Figure 5.5	:	Convergence study for cross-ply laminate (a) center deflection w' (b) center stress σ'_x	37
Figure 5.6	:	Distribution of (a) center deflection $w'\big\|_{\bar{y}=0}$ and (b) center stress $\sigma'_x\big\|_{\bar{y}=0}$ along the dimensionless plate coordinate $\bar{x}$	37
Figure 6.1	:	Isotropic square plate subjected to uniform pulse loading.....	40
Figure 6.2	:	Center deflection w' of the cross-ply laminate in time τ	41
Figure 6.3	:	Center deflection of the angle-ply laminate in time.....	42

LIST OF SYMBOLS

$A_{i,j}$, $B_{i,j}$, $D_{i,j}$	:	extensional, flexural extensional, and flexural stiffnesses
a, b	:	plate planform dimensions of x, y directions
E_1, E_2	:	layer elastic moduli in directions along fibers and normal to them, respectively
G_{12}, G_{13}, G_{23}	:	layer in-plane and thickness shear moduli
h	:	thickness of the plate
I_0	:	normal inertia coefficient per unit midplane area
I_1	:	rotatory-normal coupling inertia coefficient per unit midplane area
I_2	:	rotatory inertia coefficient per unit midplane area
K	:	shear correction coefficient
M_x, M_y, M_{xy}	:	stress couples
N_x, N_y, N_{xy}	:	in-plane stress resultants
Q_x, Q_y	:	shear stress resultants
Q_{ij}	:	reduced stiffness coefficients
q_o	:	lateral load intensity
u, v, w	:	displacement components in x, y, z directions, respectively
x, y, z	:	position coordinates in Cartesian system
γ, β	:	parameters in the Newmark time integration scheme
ε_x, ε_y, γ_{xy}, γ_{xz}, γ_{yz}	:	strain components
κ_x, κ_y, κ_{xy}	:	midplane curvatures and twist of the plate
ν	:	Poisson's ratio
ξ, η	:	width to thickness and length to thickness ratios
$\rho^{(i)}$	:	material density of the ith layer
σ_x, σ_y	:	in-plane stress components in x and y directions, respectively
ϕ_x, ϕ_y	:	rotations about the y and x axes, respectively
Φ_i	:	weight functions
ψ	:	aspect ratio of the plate ($= a/b$)

DYNAMIC NONLINEAR BEHAVIOR OF COMPOSITE PLATES

SUMMARY

Employing Galerkin technique, analyses on the dynamic nonlinear behavior of composite plates are performed in the course of this study. Large deflection of plates is investigated. Here, the magnitude of the deflections that are dealt with is of the same order as the thickness of the laminates. Hence, geometric nonlinear problem of the laminates is of interest.

First order shear deformation theory and von Kármán type nonlinearity are utilized and the governing differential equations are solved by choosing suitable polynomials as trial functions to approximate the plate displacement functions. The Galerkin method along with Newton–Raphson method is applied to large deflection analysis of laminated composite plates with various edge conditions. Dynamic large deflection analysis of composite plates is investigated using the Galerkin and the Newton-Raphson methods with Newmark direct time integration scheme.

The solutions are compared to that of Chebyshev series and finite elements. A very close agreement has been observed with these approximating methods. In the solution process, analytical computation has been done wherever it is possible, and analytical-numerical type approach has been made for all problems.

KOMPOZİT PLAKLARIN DİNAMİK NONLİNEER DAVRANIŞI

ÖZET

Bu çalışma kapsamında Galerkin yöntemi kullanılarak kompozit plakların dinamik nonlineer davranışları üzerine analizler gerçekleştirildi. Plakların büyük çökmeleri incelendi. Burada ele alınan çökmeler, katmanlı plakların kalınlıkları mertebesindedir. Dolayısıyla katmanlı plakların geometrik nonlineer problemi söz konusudur.

Birinci dereceden kayma şekil değiştirmesi teorisi ve von Kármán tipi nonlineerlik kullanıldı ve olayı yöneten diferansiyel denklemler, uygun polinomların plak yer değiştirme fonksiyonlarına yaklaşımı için seçilmesi ile çözüldü. Galerkin yöntemi Newton-Raphson yöntemi ile beraber değişik sınır şartları altındaki katmanlı kompozit plakların büyük çökme analizine uygulandı. Galerkin ve Newton-Raphson yöntemleri Newmark doğrudan zaman integrasyonu yöntemiyle beraber kullanılarak kompozit plakların dinamik büyük çökme analizleri araştırıldı.

Elde edilen çözümler Chebyshev serileri ve sonlu elemanlar yöntemlerinin çözümleri ile karşılaştırıldı. Bu yaklaşım yöntemlerinin sonuçları ile uyum içinde kalındığı gözlendi. Çözüm aşamasında mümkün olduğunca işlemler analitik olarak yapıldı ve bütün problemlerde analitik-sayısal tip yaklaşım uygulandı.

1. INTRODUCTION

1.1 Description of the Problem

In recent years, the use of laminated plates as structural members has increased considerably. Due to their light weight and high stiffness, they have been used widely in many engineering applications such as aircraft, missile, shipbuilding, auto industries, and building construction. The correct and effective use of such laminates requires more complex analysis in order to predict accurately the elastic response of these structures under external loading.

Geometric nonlinear analysis of composite plates including nonlinear bending, postbuckling, and nonlinear dynamic response (large amplitude vibration, nonlinear transient response, and wave propagation involving large deflections) is considerably more complicated than that of isotropic plates. This is because fiber-reinforced material properties and lamination geometry (fiber orientation and stacking sequence) have to be taken into account. In the case of unsymmetric laminates the existence of bending-stretching coupling complicates the problem. There are some other effects which further complicate the nonlinear analysis and hence the understanding of the elastic composite plate response. These effects include; transverse shear deformation, rotatory and in-plane inertia, transverse normal stress, initial in-plane stress, geometric imperfection, cutouts, nonclassical boundary conditions, elastic foundations, nonrectangular plate geometry. The shear deformation effect and inertia considerations are in the course of this thesis work, all the other effects are left for further research.

Static and dynamic transient response of the rectangular composite laminates under uniform lateral loads and prescribed boundary conditions are considered in this thesis work. Here, the magnitude of the deflections that are dealt with is of the same order as the thickness of the laminates. Hence, geometric nonlinear problem of the laminates is of interest, where large deflections occur and bending-stretching coupling has to be taken into account.

1.2 Definitions

1.2.1 Composite laminate

In this thesis, a composite plate will be made up of a number of perfectly bonded layers (see Fig. 1.1). Each layer (or lamina) composed of unidirectionally fiber-reinforced material is considered as a homogeneous orthotropic lamina [1]. The orthotropic axes of symmetry in each lamina of arbitrary thickness and elastic properties are oriented at an arbitrary angle to the plate axes. Two of the important types in arrangement are angle-ply and cross-ply laminates. The former is composed of layers with orthotropic axes of symmetry in each lamina alternately oriented at angles $+\theta$ and $-\theta$ with respect to the plate axes and the latter at angles of 0° and 90°.

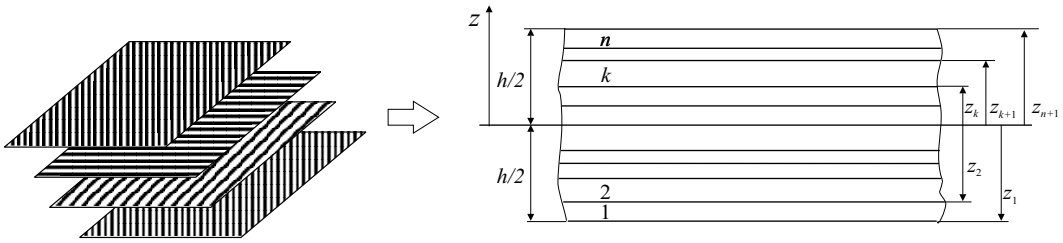


Figure 1.1: n-layered composite laminate.

1.2.2 Types of loading in dynamic analysis

The type of the solution technique in the dynamic analysis depends on the characteristic of the forcing function $P(t)$. All forcing functions can be classified into one of four types [2].

Periodic forcing function: The force amplitude repeats itself regularly many times. This is illustrated in Fig. 1.2 (a, b). The simplest form of this is a sine or cosine wave, where the force is said to be harmonic (see Fig. 1.2 (a)). A periodic function can be decomposed into a series of sine and cosine components by means of a Fourier series. For a linear system the response of each component in the Fourier series can be found separately and superposition used to add these together to give the total response. Because a periodic forcing function repeats itself many times, any initial start up transient response is not significant and is usually ignored. Instead, the steady state response, that the system settles down to is of interest. The most efficient solution methods for periodic forcing functions are those that calculate the steady state response directly. This is usually done

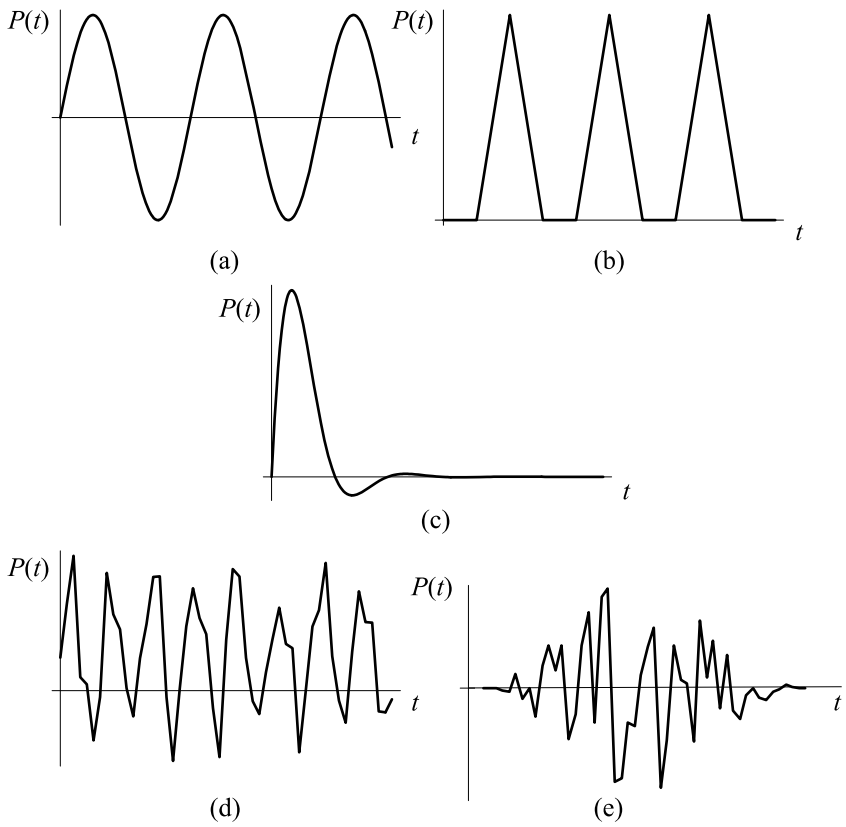


Figure 1.2: a) Harmonic. b) Periodic. c) Transient. d) Stationary random. e) Non-stationary random.

in terms of the harmonic response in the frequency domain for each frequency in the Fourier series rather than in the time domain.

Transient forcing function: In this case the force varies with time but it does not repeat itself continuously. An example of a transient forcing function is shown in Fig. 1.2 (c). Typically the force rises from zero to a maximum or a series of maxima and minima as it oscillates until it settles down to a constant value. This steady value might or might not be zero. The force is described in terms of its time history and the time history of the response is also calculated. This is carried out in the time domain. For a transient response the peak values of displacements and stresses are normally of interest and these usually occur early in the response calculation, which is another reason for conducting the calculation in the time domain.

Stationary random forcing function: In this case the force is not known precisely. If sample of the force is taken and then a second nominally identical sample taken, the two traces have the same characteristics but they are not exactly the same. In order to describe a random force, quantities such as its mean, mean

square and autocorrelation (the mean of the product of the force at two different times) are used. If the statistical quantities are constant from sample to sample then the force is said to be stationary (Fig. 1.2 (d)). A stationary random force has many characteristics of the periodic deterministic forcing function and is also solved in the frequency domain. The solution methods that are used for finding the deterministic steady state periodic response are also used, with slight modifications, for calculating the stationary random response.

Non-stationary random forcing function: Some random forces start from a low level, build up to a maximum and then die away again to a low level. Such a function is non-stationary random (see Fig. 1.2 (e)). A typical forcing function of this type is a seismic (earthquake) event. Exact solution methods for non-stationary loadings are not well developed. Instead some approximate solution techniques have been developed.

1.3 Literature Review

A considerable amount of research work has been carried out on the elastic behavior of laminated plates. Among the published works, von Kármán plate theory has gathered the most attention for the nonlinear responses of plates going under large deflection. A number of studies have been carried out concerning the large deflection analysis of plates, and a comprehensive list of papers published in the area is given in references [3–5].

For the solution of coupled, nonlinear partial differential equations, many procedures (such as finite elements, Fourier series, Rayleigh-Ritz, Galerkin) have been used. Among the method of weighted residuals, the Galerkin method (GM) is a powerful numerical solution technique to differential equations. This method involves the direct use of the differential equations (or variational form, i.e., virtual work), so it does not need the existence of a functional [6, 7]. The trial functions do not need to satisfy all the boundary conditions, and this gives flexibility to the method, which can be applied to a broad class of problems phrased in terms of integral and other types of functional equations.

The Galerkin technique has found a research area for a particular case of boundary conditions and trial functions for large deflection analysis [8–15]. Ray *et al.* [8] analyzed large deflections of simply supported rhombic plates using Galerkin technique and one-term trigonometric function for the displacement approximation. Nonlinear vibrations of arbitrarily laminated thin plates has

been treated by Woo and Nair using Galerkin method [9]. Woo and Nair assumed displacement solution in the form of double Fourier series and also utilized beam eigenfunctions. Using a displacement based higher-order theory and Galerkin procedure, Savithiri and Varadan investigated the geometrically nonlinear behavior of laminates [10]. They employed trigonometric functions for the displacement field assumption. Liu *et al.* [11] solved the problem of large deflections for symmetrically laminated elliptical plates with transverse shear deformation making use of the Galerkin method. Therein one-term polynomial functions were used for the displacement approximations. Geometrically nonlinear laminated shallow shell equations including parabolic transverse shear deformation were solved by Dennis [12]. Dennis presented a Galerkin solution to nonlinear equations assuming trigonometric functions for the shell displacements. Dumir and Dube [14] performed an approximate closed-form analytical solution of the geometrically nonlinear, axisymmetric, moderately large deflection response of a polar orthotropic, moderately thick, annular plate with a free hole and elastically constrained outer edge. They neglected the rotational and in-plane inertia and formulated the geometrically nonlinear first order shear deformation theory in terms of deflection, rotation and the stress function. They applied the Galerkin method to the equations of motion through approximating the rotation by a one-term polynomial function.

Different numerical techniques were employed to investigate the geometrically nonlinear behavior of plates. Large deflection of unsymmetric laminates was analyzed with perturbation method by Chia and Prabhakara [16]. Pica *et al.* solved the large deflection problem of isotropic plates using finite element technique [17]. Reddy and Chao applied the finite element method (FEM) to large deflection and large amplitude free vibration problems of laminates [18]. Turvey and Osman performed the large deflection analysis of isotropic plates using Dynamic Relaxation technique [19]. Geometrically nonlinear flexural response of unsymmetrically laminated composite plates was investigated by Singh *et al.* [20]. They employed a higher order theory and developed a four-node rectangular C^1 continuous finite element having 14 degrees of freedom per node. Bencharif and Ng [21] conducted nonlinear analysis of thick rectangular plates using general three-dimensional equations and applied finite difference technique to the governing nonlinear equations. Based on the Reissner-Mindlin plate theory and using Galerkin-perturbation technique, a nonlinear bending analysis of plates resting on elastic foundations was presented by Shen [22]. Using Chebyshev polynomials (CP) Shukla and Nath investigated the large deflection of moderately thick laminated rectangular plates [23]. Liew et al. proposed a mesh-free kp-Ritz

method for the large deflection flexural analysis of laminated composite plates [24]. The first order shear deformation theory and von Kármán type nonlinearity are employed in [23] and [24].

For the geometrically nonlinear dynamic response of laminated composite various numerical techniques can be utilized. Bauer solved the nonlinear transient problem of the isotropic plates using a proper stress function and applying the Ritz-Galerkin method to the deflection equation [25]. In this work, the resulting ordinary nonlinear differential equation in time was handled using a perturbation technique. Using the finite element method with Newmark time integration scheme, Reddy investigated the linear [26] and nonlinear [27] transient response of plates. Ali and Al-Noury [28] solved the nonlinear transient response of rectangular plates using an implicit finite difference method. A semi-analytical finite strip method (FSM) has been developed for analyzing nonlinear transient problem of laminates by Chen *et al.* [29]. Wang *et al.* [30] derived a formulation for strip element method to include the rotatory inertia term in the transient analysis of laminates. Nath and Shukla [31] used Chebyshev series (CS) technique for the nonlinear transient analysis of laminates. In a recent work, Chebyshev-collocation method with Newmark scheme is applied to the von Kármán plate theory by Kirby and Yosibash [32]. Here, the reviews [33, 34] on the vibrations of plates will be useful for the researchers studying the dynamic behavior of plates.

In the previous works of Tanrıöver and Şenocak [13, 15], the Galerkin method with the use of Newton-Raphson method has been applied to large deflection analysis of laminated plates with various edge conditions. Here, the von Kármán plate theory is utilized and the governing differential equations are solved by choosing suitable polynomials as trial functions to approximate the two dimensional displacement functions. The trial functions are constructed in a way that essential boundary conditions are satisfied. In the solution process, analytical computation has been done wherever it is possible, and analytical-numerical type approach has been made for all problems. The evaluations of integrals are symbolically computed by using a commercial computer math code $Mathematica^{TM}$ [35].

A recent research work on the nonlinear dynamic analysis of laminated composite plate using GM is accomplished [36, 37]. Herein, the von Kármán type nonlinearity is considered and the dynamic nonlinear analysis is performed through using the Newmark method in association with the Newton-Raphson method. The solutions are compared to that of finite strips [29].

1.4 Objectives and Scope of the Thesis Work

Geometrically nonlinear behavior of composite laminates has been investigated using the Galerkin method in the course of this thesis. Among the weighted residual methods the Galerkin method is a powerful numerical technique. In the application of the method a critical choice of the trial functions (admissible functions satisfying the geometrical boundary conditions) is needed. Herein, polynomials are chosen as the trial functions.

In some of the studies in the literature one type, and in some others limited boundary conditions are considered for the geometrically nonlinear analysis of laminated plates. This is mainly due to the arising difficulties during the solution process. However, polynomials make it easy to implement different kinds of boundary conditions. In this work, a variety of boundary conditions has been investigated and the solutions are compared to known results. An other advantage of using polynomials is; lengthy computations resulting from the governing nonlinear equations can be handled easily (in terms of manipulation and integration). Note that, in the solution process the computations have been carried out analytically wherever it is possible and analytical-numerical type approach has been made for all problems. To the best of authors knowledge, there are a few works published on the Galerkin method in which an analytical-numerical type approach is employed for such cumbersome problems. Hence, the results of this study can be used as a benchmark for comparison.

Aforementioned studies of Tanrıöver and Şenocak on geometrically nonlinear behavior of plates do not cover the shear deformation, rotatory inertia and in-plane inertia effects. Thesis works on the geometrically nonlinear behavior of composite plates are extended to first order shear deformation theory (FSDT) of moderately thick plates, where these effects are included in the analyses. Large deflection analyses of symmetric and unsymmetric laminates under various boundary conditions are performed by using the Galerkin method. The effect of thickness in the FSDT formulation is investigated. For the dynamic analyses, first, a linear transient analysis of an isotropic plate is carried out for better understanding the transient response and verification. Then the nonlinear transient analyses are performed for unsymmetric cross-ply and angle-ply laminates. Comparisons with other solution techniques are also given.

1.5 Outline of the Thesis

The thesis contains seven chapters. In the first chapter, a description of the problem, some required definitions, a literature review and objectives and scope of the thesis work are given. The concept of geometric nonlinearity and its application to the plates are introduced in the next chapter. In Chapter 3, an overview of the laminate theories is presented as a background. Chapter 4 provides the governing equations, solution technique and boundary conditions. Next, numerical examples on static and dynamic behavior of laminates are introduced and the results are given as a comparison with the other solution techniques in Chapters 5 and 6. In Chapter 7, a conclusion is given.

2. GEOMETRIC NONLINEARITY FOR PLATES

In this chapter, a brief definition of deformation of a three-dimensional body and related strain-displacement equations are outlined. Intermediate class of deformations are defined and an illustration of the corresponding deformation in a plane is presented. Lastly, assumptions and von Kármán strains for plates are given.

2.1 Displacements and Strains in a Three-Dimensional Body

The configuration of a solid body is the simultaneous position of all material particles of the body. A change in the configuration of the body is a displacement. It is assumed that the change is continuous; i.e., fractures or any new boundary surfaces are none of our concern. When portions of a body are displaced relative to one another under some physical action, the body is said to be deformed. Now, kinematics of the deformation can be presented.

Consider two points $A(x, y, z)$ and $B(x + dx, y + dy, z + dz)$ in the undeformed configuration of the body which are the end points of a differential line element ds (see Fig. 2.1). According to theorem of Pythagoras, the square of the length of this line element is given below.

$$ds^2 = dx^2 + dy^2 + dz^2 \tag{2.1}$$

When A and B are deformed to the points $A^*(x^*, y^*, z^*)$ and $B^*(x^*+dx^*, y^*+dy^*, z^* + dz^*)$, respectively, the square of the length ds^* of the new element is

$$ds^{*2} = dx^{*2} + dy^{*2} + dz^{*2}. \tag{2.2}$$

The displacement vector of the material point A is introduced as $\overrightarrow{AA^*}$ and the components of this vector is

$$u = x^* - x, \quad v = y^* - y, \quad w = z^* - z. \tag{2.3}$$

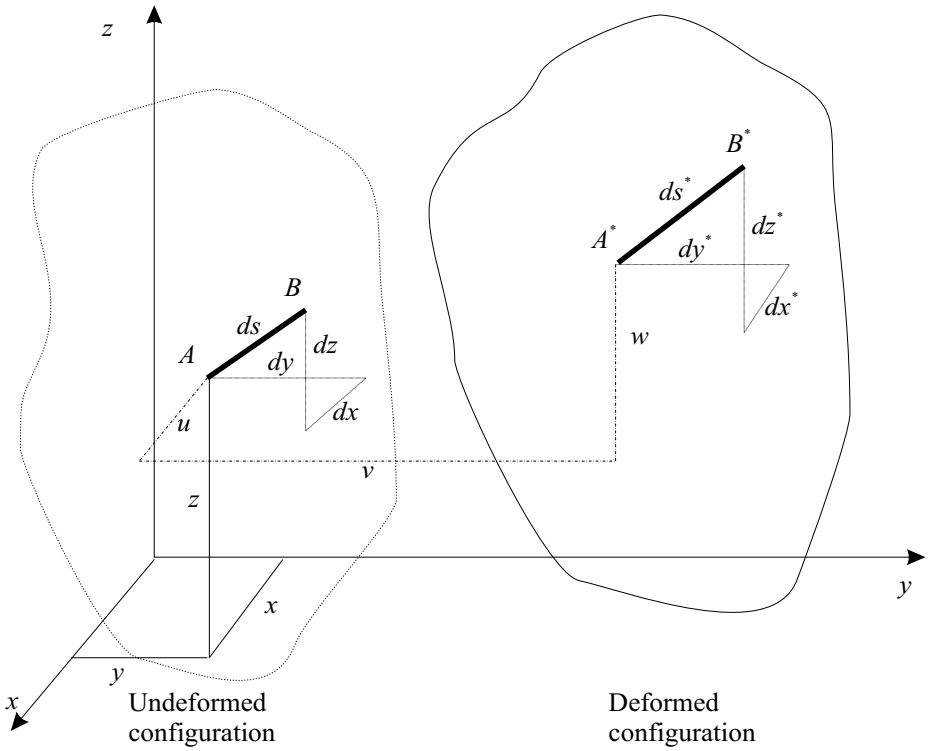


Figure 2.1: Deformation of a three-dimensional solid body.

The difference $ds^{*2} - ds^2$ can be used as a measure of deformation. This difference is rewritten with the use of Eq. (2.3) and given as

$$ds^{*2} - ds^2 = 2\,\varepsilon_x\,dx^2 + 2\,\varepsilon_y\,dy^2 + 2\,\varepsilon_z\,dz^2$$
$$+2\,\gamma_{xy}\,dx\,dy + 2\,\gamma_{xz}\,dx\,dz + 2\,\gamma_{yz}\,dy\,dz, \tag{2.4}$$

where

$$\varepsilon_x = \frac{\partial u}{\partial x} + \frac{1}{2}[(\frac{\partial u}{\partial x})^2 + (\frac{\partial v}{\partial x})^2 + (\frac{\partial w}{\partial x})^2], \tag{2.5}$$
$$\varepsilon_y = \frac{\partial v}{\partial y} + \frac{1}{2}[(\frac{\partial u}{\partial y})^2 + (\frac{\partial v}{\partial y})^2 + (\frac{\partial w}{\partial y})^2], \tag{2.6}$$
$$\varepsilon_z = \frac{\partial w}{\partial z} + \frac{1}{2}[(\frac{\partial u}{\partial z})^2 + (\frac{\partial v}{\partial z})^2 + (\frac{\partial w}{\partial z})^2], \tag{2.7}$$
$$\gamma_{xy} = \frac{\partial v}{\partial x} + \frac{\partial u}{\partial y} + \frac{\partial u}{\partial x}\frac{\partial u}{\partial y} + \frac{\partial v}{\partial x}\frac{\partial v}{\partial y} + \frac{\partial w}{\partial x}\frac{\partial w}{\partial y}, \tag{2.8}$$
$$\gamma_{xz} = \frac{\partial w}{\partial x} + \frac{\partial u}{\partial z} + \frac{\partial u}{\partial x}\frac{\partial u}{\partial z} + \frac{\partial v}{\partial x}\frac{\partial v}{\partial z} + \frac{\partial w}{\partial x}\frac{\partial w}{\partial z}, \tag{2.9}$$
$$\gamma_{yz} = \frac{\partial w}{\partial y} + \frac{\partial v}{\partial z} + \frac{\partial u}{\partial y}\frac{\partial u}{\partial z} + \frac{\partial v}{\partial y}\frac{\partial v}{\partial z} + \frac{\partial w}{\partial y}\frac{\partial w}{\partial z}. \tag{2.10}$$

Here, the quantities ε_x, ε_y, ε_z, γ_{xy}, γ_{xz} and γ_{yz} are the components of strain written in Lagrangian coordinates (see [38, 39]). These equations are referred as strain-displacement relations. In a given strain state, these relations yield a system of highly nonlinear partial differential equations in the unknown components of displacement.

2.2 Geometric Nonlinearity

If the deformation of the body is small, assumptions on the strain-displacement relations can be made. Here, the small deformation means that u, v and w displacements are small compared with characteristic dimensions of the body. In such a case, squares and products of the first partial derivatives of u, v and w are assumed negligible compared with the derivatives themselves. Hence, the well known equations of classical linear theory of elasticity are reached. Then the strains of fibers in one plane are not influenced by out-of-plane displacements, while they would be influenced if the nonlinear terms were retained.

The geometric nonlinearity in this thesis is limited to what may be called an intermediate class of deformations. To illustrate the intermediate class of deformation in a plane, a line element of length dx_1 that is initially parallel to the x axis is considered (see Fig. 2.2).

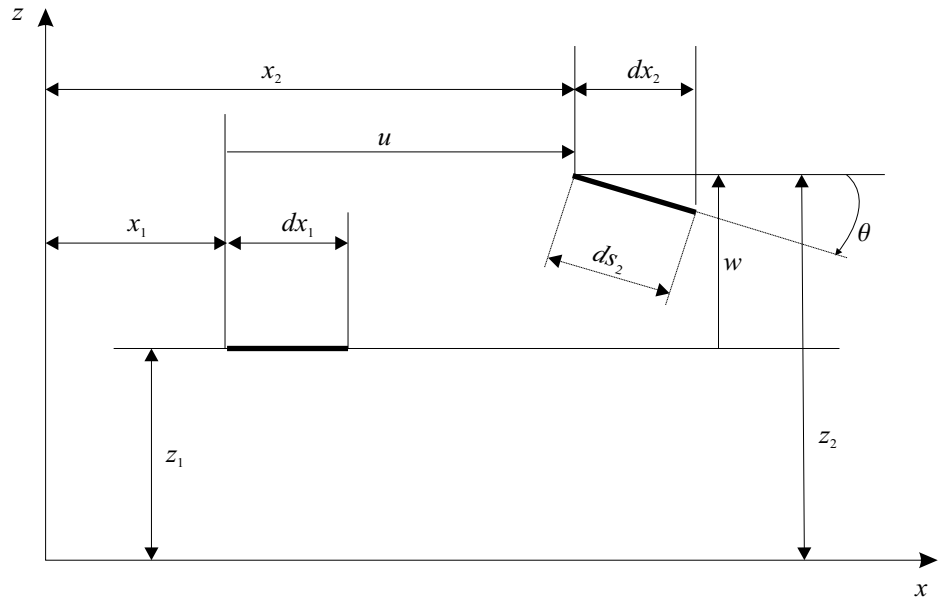


Figure 2.2: Configuration of a line element before and after deformation.

Recall from Eq. (2.3);

$$x_2 = x_1 + u, \quad z_2 = z_1 + w. \tag{2.11}$$

The differentiation with respect to x_1 gives

$$\frac{dx_2}{dx_1} = 1 + \frac{du}{dx_1}, \quad \frac{dz_2}{dx_1} = \frac{dw}{dx_1}. \tag{2.12}$$

By the Pythagorean theorem,

$$ds_2^2 = dx_2^2 + dz_2^2. \tag{2.13}$$

In another way,

$$(\frac{ds_2}{dx_1})^2 = (\frac{dx_2}{dx_1})^2 + (\frac{dz_2}{dx_1})^2 = (1 + \frac{du}{dx_1})^2 + (\frac{dw}{dx_1})^2. \tag{2.14}$$

Now a definition of an extensional strain of the line element can be written by the relation

$$\varepsilon_x = \frac{ds_2 - dx_1}{dx_1}. \tag{2.15}$$

By suitable rearrangement this expression will be

$$\varepsilon_x + \frac{1}{2}\varepsilon_x^2 = \frac{1}{2}\,[(\frac{ds_2}{dx_1})^2 - 1]. \tag{2.16}$$

In intermediate class of deformations, strains are much smaller than unity (and Hooke's law holds) that an assumption neglecting the square of ε_x will be suitable. Then the Eq. (2.16) may be replaced by the approximate relation

$$\varepsilon_x = \frac{1}{2}\,[(\frac{ds_2}{dx_1})^2 - 1]. \tag{2.17}$$

Substituting the Eq. (2.14) into the above equation gives

$$\varepsilon_x = \frac{du}{dx_1} + \frac{1}{2}\,[(\frac{du}{dx_1})^2 + (\frac{dw}{dx_1})^2]. \tag{2.18}$$

The distinguishing characteristic of the present intermediate class of deformations is that the rotation θ in Fig. 2.2 also is small (but not negligibly small). If both ε_x and $(\frac{dw}{dx_1})^2$ are small compared with unity, the $\frac{du}{dx_1}$ also is small compared with unity. Then the square of $\frac{du}{dx_1}$ may be neglected and, approximately,

$$\varepsilon_x = \frac{du}{dx_1} + \frac{1}{2}(\frac{dw}{dx_1})^2. \tag{2.19}$$

This is the strain-displacement relationship for an intermediate class of deformations in a plane (see [40] for details).

2.2.1 Large deflection of a plate

A plate is a body bounded by two surfaces of small curvature, the distance between these surfaces, called the thickness, being small in comparison with the dimensions of the surface (see Fig. 2.3). The thickness of the plate will be denoted by h. A surface equidistant to the bounding surfaces is called the middle surface. When the thickness is constant, the plate is said to be of uniform thickness. When the middle surface is a plane in the undeformed configuration, the plate is said to be flat. In the scope of this thesis only flat plates of uniform thickness and of linear elastic material will be considered.

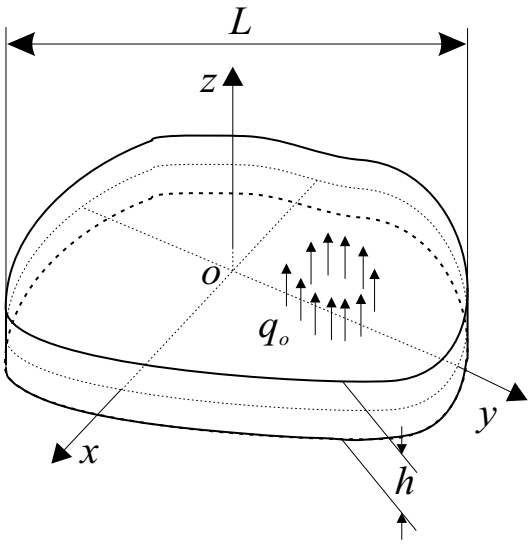


Figure 2.3: A plate with a coordinate system and dimensions.

If sufficiently high intensity of lateral load q_o is applied, a strong bending of plate that leads to large deflection can be provided. Here, the large deflection of the plate is an intermediate class of deformation; the magnitude of the deflection w

is of the same order as the thickness of the plate, h, but small compared with the typical plate dimension L. Also, the slopes $\frac{\partial w}{\partial x}$ and $\frac{\partial w}{\partial x}$ are moderate. For the large deflection of plates the strain-displacement relationship can be obtained by modifying the Eqs. (2.5–2.10) and given as

$$\varepsilon_x = \frac{\partial u}{\partial x} + \frac{1}{2}\left(\frac{\partial w}{\partial x}\right)^2, \tag{2.20}$$

$$\varepsilon_y = \frac{\partial v}{\partial y} + \frac{1}{2}\left(\frac{\partial w}{\partial y}\right)^2, \tag{2.21}$$

$$\varepsilon_z = \frac{\partial w}{\partial z}, \tag{2.22}$$

$$\gamma_{xy} = \frac{\partial v}{\partial x} + \frac{\partial u}{\partial y} + \frac{\partial w}{\partial x}\frac{\partial w}{\partial y}, \tag{2.23}$$

$$\gamma_{xz} = \frac{\partial w}{\partial x} + \frac{\partial u}{\partial z}, \tag{2.24}$$

$$\gamma_{yz} = \frac{\partial w}{\partial y} + \frac{\partial v}{\partial z}, \tag{2.25}$$

where, these equations are referred as von Kármán strains [41].

3. AN OVERVIEW OF LAMINATED PLATE THEORIES

At the present time many of the existing methods of analysis for multilayered anisotropic plates and shells are direct extensions of those developed earlier for homogeneous isotropic and orthotropic plates and shells. A review of the theory of elastic plates can be found in the literature [42–44].

Laminated composite structures are made up of layers of orthotropic materials that are bonded together. The layers may be of different materials, or of the same orthotropic material, with the principal material directions of each layer oriented at different angles to the reference axes. By altering the material or orientation, or both, of each layer, a structural designer can tailor the strength and other properties of a laminate to the requirements of a given application.

The analysis of fiber-reinforced, laminated composite structures presents many modelling challenges. For example, the global deformation of laminated composite structures is often characterized by complex coupling between the extension, bending and shearing modes (see [1, 5, 45–47]). Due to their low transverse shear stiffness, composite laminates often exhibit significant transverse shear deformation at lower thickness to span ratios than do similar homogeneous isotropic plates and shells. At the ply level, laminated composites often exhibit stress concentrations near material and geometric discontinuities that can lead to damage in the form of delamination, matrix cracking and adhesive bond separation.

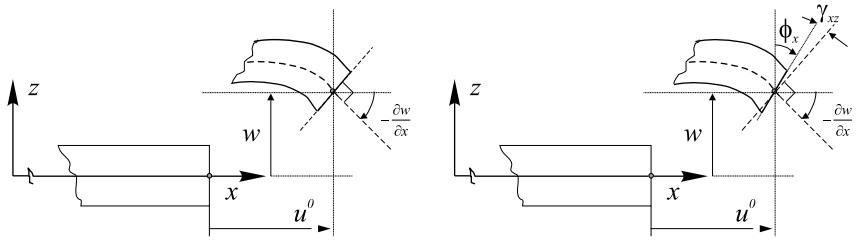
One of the important steps to develop accurate analysis of laminated composite plates is to select a proper structure theory. Actually, several laminate models are available in the literature. In particular, two different approaches may be distinguished in the laminate modelling, which lead to two classes of laminate theories: the equivalent single layer theories (ESLTs) and the layerwise theories (LWTs).

3.1 Single Layer Theories

The ESLTs are those in which a heterogeneous laminated plate or shell is treated as a statically equivalent, single layer having complex constitutive behavior, reducing the 3–D continuum problem to a 2–D one [48]. The ESLTs are developed by assuming that the displacement field is at least C^1–continuous (i.e., the function and its derivative are continuous) through the thickness of the laminate.

When the main emphasis of the analysis is to determine the overall global response of the laminated component, for example, gross deflections, critical buckling loads, fundamental vibration frequencies, and associated mode shapes, such global behavior can often be accurately determined using relatively simple ESLTs. However, the equivalent single layer models have several serious limitations that prevent them from being used to solve the whole spectrum of composite laminate problems. First, the accuracy of the global response predicted by the ESLTs deteriorates as the laminate becomes thicker. Second, the ESLTs are often incapable of accurately describe the state of stress and strain at the ply level near geometric and material discontinuities or near regions of intense loading. Finally, equivalent single layer models can not model the kinematics of delamination.

Two commonly used examples of simple ESLTs are the classical laminated plate theory (CLPT) and first order shear deformation theory.



(a) (b)

Figure 3.1: a) Classical laminated plate theory. b) First order shear deformation theory.

3.1.1 Classical laminated plate theory

The laminate is presumed to consist of perfectly bonded laminae. Moreover, the bonds are presumed to be infinitesimally thin as well as non-shear deformable.

That is, the displacements are continuous across lamina boundaries so that no lamina can slip relative to another.

Accordingly, if laminate is thin, a line originally straight and perpendicular to the middle surface of the laminate, i.e., a normal to the middle surface, is assumed to remain straight and perpendicular to the middle surface when the laminate is deformed (see Fig. 3.1 (a)). Requiring the normal to the middle surface to remain straight and normal under deformation is equivalent to ignoring the shearing strains in planes perpendicular to the middle surface, that is, $\gamma_{xz} = \gamma_{yz} = 0$. In addition the normals are presumed to have constant length so that the strain perpendicular to the middle surface is ignored as well, that is $\varepsilon_z = 0$. The foregoing collection of assumptions of the behavior of the single layer that represents the laminate constitutes the familiar Kirchhoff hypothesis for plates [5, 46]. The laminate strains have been reduced to ε_x, ε_y and γ_{xy} by virtue of the Kirchhoff hypothesis, that is ε_z, γ_{xz} and γ_{yz} vanished.

Kirchhoff hypothesis implies

$$u(x, y, z, t) = u^0(x, y, t) - z\,\frac{\partial w}{\partial x}, \tag{3.1}$$

$$v(x, y, z, t) = v^0(x, y, t) - z\,\frac{\partial w}{\partial y}, \tag{3.2}$$

$$w(x, y, z, t) = w^0(x, y, t), \tag{3.3}$$

where $u^0(x, y)$, $v^0(x, y)$ and $w^0(x, y)$ are middle surface displacements.

3.1.2 First order shear deformation theory

The first order shear deformation theory is an extension of the Reissner [49, 50], and Mindlin [51], plate models to the case of laminated anisotropic plates. An extension of the FSDT to laminates was originally due to Yang, Norris and Stavsky [52]. Having low transverse elasticity modulus compared to inplane elasticity modulus increases the importance of shear deformation effect in laminated composite plates [53].

The FSDT still remains the most widely used theory for anisotropic laminated plates in engineering applications owing to its simplicity and low computational cost (see, for example, [54–56]). Literature survey on shear deformation theories for composite plates can be found in references [57–60].

The FSDT extends the kinematics of the CLPT by including a gross transverse shear deformation in its kinematic assumptions (see Fig. 3.1 (b)). The displacement field of the FSDT is of the form

$$u(x, y, z, t) = u^0(x, y, t) + \phi_x(x, y, t)\, z, \tag{3.4}$$

$$v(x, y, z, t) = v^0(x, y, t) + \phi_y(x, y, t)\, z, \tag{3.5}$$

$$w(x, y, z, t) = w^0(x, y, t), \tag{3.6}$$

where $(u^0, v^0, w^0, \phi_x, \phi_y)$ are unknown functions to be determined. Note that the strains $(\varepsilon_x, \varepsilon_y, \gamma_{xy})$ are linear through the laminate thickness, while the transverse shear strains $(\gamma_{xz}, \gamma_{yz})$ are constant.

Since the transverse shear strains are represented as constant through the laminate thickness, it follows that the transverse shear stresses will also be constant. It is well known from elementary theory of homogenous beams that the transverse shear stress varies parabolically through the beam thickness. In composite laminated beams and plates, the transverse shear stresses vary at least quadratically through the layer thickness. This discrepancy between the actual stress state and the constant stress state predicted by the FSDT is often corrected in computing the transverse shear force resultants (Q_x, Q_y) by multiplying the corresponding integrals with a parameter K, called shear correction coefficient (see [5, 46]):

$$\begin{Bmatrix} Q_y \\ Q_x \end{Bmatrix} = K \int_{-h/2}^{h/2} \begin{Bmatrix} \sigma_{xz} \\ \sigma_{yz} \end{Bmatrix} dz, \tag{3.7}$$

where σ_{xz} and σ_{yz} are transverse shear stresses.

3.1.3 Higher order theories

The CLPT and the FSDT are the simplest ESLTs, and they adequately describe the kinematic behavior of most laminates. Higher order theories can represent the kinematics better, may not require shear correction coefficients, and can yield more accurate interlaminar stress distributions. However, they involve considerably more computational effort [5].

Higher order ESLTs use higher order polynomials in the expansion of the displacement components through the thickness of the laminate (see, for example,

[61–65]). The second order third order theories introduce additional unknowns that are difficult to interpret in physical terms. The general third order theory is based on the displacement field [61, 62]:

$$u(x,y,z,t) = u^0(x,y,t) + \phi_x(x,y,t)\,z + \psi_x(x,y,t)\,z^2 + \theta_x\,z^3, \tag{3.8}$$

$$v(x,y,z,t) = v^0(x,y,t) + \phi_y(x,y,t)\,z + \psi_y(x,y,t)\,z^2 + \theta_y\,z^3, \tag{3.9}$$

$$w(x,y,z,t) = w^0(x,y,t) + \phi_z(x,y,t)\,z + \psi_z\,z^2, \tag{3.10}$$

where $(u^0, v^0, w^0, \phi_x, \phi_y, \phi_z, \psi_x, \psi_y, \psi_z, \theta_x, \theta_y, \theta_z)$ are unknown functions. It is clear that (u^0, v^0, w^0) and (ϕ_x, ϕ_y) have the same physical meaning as in the first order theory; they denote the displacements and rotations of transverse normals on the plane $z = 0$, respectively:

$$\begin{aligned} &u^0 = u(x,y,0,t), \quad v^0 = v(x,y,0,t), \\ &w^0 = w(x,y,0,t), \\ &\phi_x = \frac{\partial u}{\partial z}(x,y,0,t), \quad \phi_y = \frac{\partial v}{\partial z}(x,y,0,t). \end{aligned} \tag{3.11}$$

The function ϕ_z has the meaning of extension of a transverse normal, and the remaining functions can be interpreted as higher order rotations that specify the deformed shape of a straight line perpendicular to the reference plane in the undeformed plate.

The third order theories provide a slight increase in accuracy relative to the FSDT solution, at the expense of a significant increase in computational effort. Theories higher than third order are not used because the accuracy gained is so little that the effort required to solve the equations is not justified [48].

3.2 Layerwise Theories

In contrast to the ESLTs, the LWTs are developed by assuming that the displacement field exhibits only C^0–continuity through the laminate thickness. Thus the displacement components are continuous through the laminate thickness but the derivatives of the displacements with respect to the thickness coordinate may be discontinuous at various points through the thickness, thereby allowing for the possibility of continuous transverse stresses at interfaces separating dissimilar materials. Layerwise displacement fields provide a

much more kinematically correct representation of the moderate to severe cross-sectional warping associated with the deformation of thick laminates.

The imposition of the continuity of transverse stresses at layer interfaces can be used to reduce the total number of generalized displacement parameters in the theory. For example, a simplified layerwise theory with only five generalized displacements for describing the deformation of the plate is obtained by assuming the in-plane displacements to be piecewise linear in the thickness coordinate z, and the transverse displacement w to be independent of z. Di Sciuva [66] used these ideas to formulate a displacement based theory, called the zigzag theory or discrete-layer theory. The displacement field is assumed to be of the form

$$u(x,y,z,t) = u^0(x,y,t) - \frac{\partial w}{\partial x}(x,y,t)\, z + f_{11}(z)\phi_1(x,y,t) + f_{12}(z)\phi_2(x,y,t), \tag{3.12}$$

$$v(x,y,z,t) = v^0(x,y,t) - \frac{\partial w}{\partial y}(x,y,t)\, z + f_{21}(z)\phi_1(x,y,t) + f_{22}(z)\phi_2(x,y,t), \tag{3.13}$$

$$w(x,y,z,t) = w^0(x,y,t). \tag{3.14}$$

The functions f_{ij} and ϕ_i $(i,j = 1,2)$ can then be determined such that the displacements and transverse stresses are continuous at layer interfaces. The resulting laminate theory contains only five dependent unknowns, as in the FSDT. Such LWTs are referred to as partial LWTs since the transverse normal displacement does not have a layerwise representation. Several other LWTs are presented by researchers (see, for example, [67, 68]).

In contrast to the partial LWTs, full LWTs use layerwise expansions for all three displacement components, and thus include both discrete layer transverse shear effects and discrete layer transverse normal effects. Many of the cited theories can be considered as special cases of a general theory based on the following through-the-thickness displacement assumptions in the kth layer (see [69]):

$$u^k(x,y,z,t) = \sum_{j=1}^{n} u_j^k(x,y,t)\, \psi_j^k(z), \tag{3.15}$$

$$v^k(x,y,z,t) = \sum_{j=1}^{n} v_j^k(x,y,t)\, \psi_j^k(z), \tag{3.16}$$

$$w^k(x,y,z,t) = \sum_{j=1}^{n} w_j^k(x,y,t)\,\psi_j^k(z), \tag{3.17}$$

where u^k, v^k and w^k represent the total displacement components in the x, y and z directions, respectively, and $\psi_j^k(z)$ are continuous functions of the thickness coordinate.

Since LWTs are out of the scope of this thesis, further details will not be given here. A recent review of the LWTs presented by Carrera [70] can be useful to carry out more detailed research on this topic.

4. GEOMETRICALLY NONLINEAR BEHAVIOR OF MODERATELY THICK LAMINATED COMPOSITE PLATES

Geometrically nonlinear behavior of moderately thick laminated plates considering the von Kármán type nonlinearity is presented. The first order shear deformation theory based on Mindlin's hypothesis is employed. Governing nonlinear equations are solved using the GM in association with the Newton-Raphson method.

4.1 Governing Equations

Consider a rectangular laminated plate with dimensions a, b and uniform thickness h. The origin of the coordinate system is chosen to coincide with the center of the midplane of the undeformed plate (see Fig. 4.1). The plate is assumed to be subjected uniform transverse pressure q_o, and it is constructed of finite homogenous orthotropic layers perfectly bonded together.

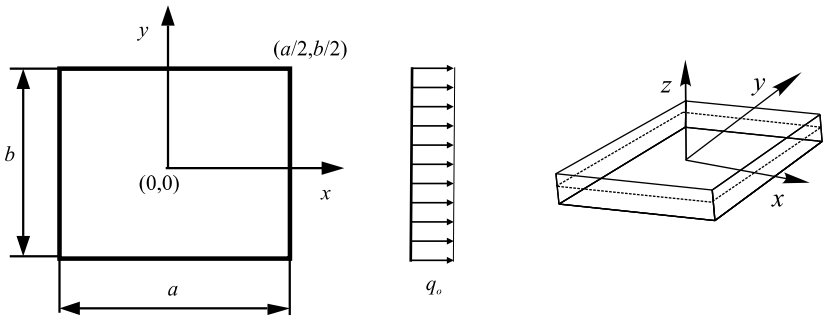


Figure 4.1: Plate geometry and loading.

Under the assumptions of first order shear deformation theory and geometric nonlinearity in the von Kármán sense [40]; let u, v, w denote the displacements at an arbitrary point of the plate in the x, y, z directions and $u^0(x,y)$, $v^0(x,y)$, $w^0(x,y)$ are the displacements at a corresponding point of the midplane of the plate in the x, y and z directions respectively. Then the displacement field of the first order theory is of the form

$$u(x,y,z,t) = u^0(x,y,t) + \phi_x(x,y,t)\, z, \tag{4.1}$$

$$v(x,y,z,t) = v^0(x,y,t) + \phi_y(x,y,t)\, z, \tag{4.2}$$

$$w(x,y,z,t) = w^0(x,y,t) \tag{4.3}$$

where ϕ_x and ϕ_y are the rotations of a transverse normal about the y and x axes respectively (see Fig. 3.1 (b)). The corresponding total strains could be expressed as follows:

$$\varepsilon_x = \varepsilon_x^0 + \kappa_x z, \tag{4.4}$$

$$\varepsilon_y = \varepsilon_y^0 + \kappa_y z, \tag{4.5}$$

$$\gamma_{xy} = \gamma_{xy}^0 + \kappa_{xy} z, \tag{4.6}$$

$$\gamma_{xz} = \gamma_{xz}^0, \tag{4.7}$$

$$\gamma_{yz} = \gamma_{yz}^0. \tag{4.8}$$

Considering von Kármán type geometric nonlinearity, the strain displacement relations can be written as

$$\varepsilon_x^0 = u_{,x}^0 + \frac{1}{2} w_{,x}^2, \tag{4.9}$$

$$\varepsilon_y^0 = v_{,y}^0 + \frac{1}{2} w_{,y}^2, \tag{4.10}$$

$$\gamma_{xy}^0 = u_{,y}^0 + v_{,x}^0 + w_{,x} w_{,y}, \tag{4.11}$$

$$\gamma_{xz}^0 = w_{,x} + \phi_x, \tag{4.12}$$

$$\gamma_{yz}^0 = w_{,y} + \phi_y, \tag{4.13}$$

where differentiations are denoted by comma. Midplane curvatures and twist of the plate are the following:

$$\kappa_x = \phi_{x,x}, \tag{4.14}$$

$$\kappa_y = \phi_{y,y}, \tag{4.15}$$

$$\kappa_{xy} = \phi_{x,y} + \phi_{y,x}. \tag{4.16}$$

The strains can be written as

$$\begin{Bmatrix} \varepsilon_x \\ \varepsilon_y \\ \gamma_{yz} \\ \gamma_{xz} \\ \gamma_{xy} \end{Bmatrix} = \begin{Bmatrix} u^0_{,x} + \frac{1}{2}w^2_{,x} \\ v^0_{,y} + \frac{1}{2}w^2_{,y} \\ w_{,y} + \phi_y \\ w_{,x} + \phi_x \\ u^0_{,y} + v^0_{,x} + w_{,x}w_{,y} \end{Bmatrix} + z \begin{Bmatrix} \phi_{x,x} \\ \phi_{y,y} \\ 0 \\ 0 \\ \phi_{x,y} + \phi_{y,x} \end{Bmatrix}, \tag{4.17}$$

or

$$\begin{Bmatrix} \varepsilon_x \\ \varepsilon_y \\ \gamma_{yz} \\ \gamma_{xz} \\ \gamma_{xy} \end{Bmatrix} = \begin{Bmatrix} \varepsilon^0_x \\ \varepsilon^0_y \\ \gamma^0_{yz} \\ \gamma^0_{xz} \\ \gamma^0_{xy} \end{Bmatrix} + z \begin{Bmatrix} \varepsilon^1_x \\ \varepsilon^1_y \\ \gamma^1_{yz} \\ \gamma^1_{xz} \\ \gamma^1_{xy} \end{Bmatrix}. \tag{4.18}$$

For a plate with an arbitrary number of layers, the constitutive relations are

$$\begin{Bmatrix} N_x \\ N_y \\ N_{xy} \end{Bmatrix} = \begin{bmatrix} A_{11} & A_{12} & A_{16} \\ A_{12} & A_{22} & A_{26} \\ A_{16} & A_{26} & A_{66} \end{bmatrix} \begin{Bmatrix} \varepsilon^0_x \\ \varepsilon^0_y \\ \gamma^0_{xy} \end{Bmatrix} + \begin{bmatrix} B_{11} & B_{12} & B_{16} \\ B_{12} & B_{22} & B_{26} \\ B_{16} & B_{26} & B_{66} \end{bmatrix} \begin{Bmatrix} \kappa_x \\ \kappa_y \\ \kappa_{xy} \end{Bmatrix}, \tag{4.19}$$

$$\begin{Bmatrix} M_x \\ M_y \\ M_{xy} \end{Bmatrix} = \begin{bmatrix} B_{11} & B_{12} & B_{16} \\ B_{12} & B_{22} & B_{26} \\ B_{16} & B_{26} & B_{66} \end{bmatrix} \begin{Bmatrix} \varepsilon^0_x \\ \varepsilon^0_y \\ \gamma^0_{xy} \end{Bmatrix} + \begin{bmatrix} D_{11} & D_{12} & D_{16} \\ D_{12} & D_{22} & D_{26} \\ D_{16} & D_{26} & D_{66} \end{bmatrix} \begin{Bmatrix} \kappa_x \\ \kappa_y \\ \kappa_{xy} \end{Bmatrix}, \tag{4.20}$$

$$\begin{Bmatrix} Q_y \\ Q_x \end{Bmatrix} = K \begin{bmatrix} A_{44} & A_{45} \\ A_{45} & A_{55} \end{bmatrix} \begin{Bmatrix} \gamma^0_{yz} \\ \gamma^0_{xz} \end{Bmatrix}, \tag{4.21}$$

where N_x, N_y and N_{xy} are the resultant in-plane, Q_x and Q_y are transverse forces and M_x, M_y and M_{xy} are moments conjugate to in-plane strains (ε^0_x, ε^0_y, γ^0_{xy}), transverse shear strains (γ^0_{yz}, γ^0_{xz}) and curvatures (κ_x, κ_y, κ_{xy}) respectively. Resultant forces and moments are defined as

$$\begin{Bmatrix} N_x \\ N_y \\ N_{xy} \end{Bmatrix} = \int_{-h/2}^{h/2} \begin{Bmatrix} \sigma_x \\ \sigma_y \\ \sigma_{xy} \end{Bmatrix} dz, \quad \begin{Bmatrix} M_x \\ M_y \\ M_{xy} \end{Bmatrix} = \int_{-h/2}^{h/2} \begin{Bmatrix} \sigma_x \\ \sigma_y \\ \sigma_{xy} \end{Bmatrix} z\, dz, \tag{4.22}$$

where $(\sigma_x, \sigma_y, \sigma_{xy})$ are in-plane stresses. The parameter K introduced in the Eq. (4.21) is shear correction coefficient. A_{ij}, B_{ij} and D_{ij} are symmetric matrices defined as follows:

$$(A_{ij}, B_{ij}, D_{ij}) = \int_{-h/2}^{h/2} (1, z, z^2)\, Q_{ij}\, dz, \tag{4.23}$$

where Q_{ij} is the corresponding reduced stiffness coefficients.

The governing equations of motion of the FSDT can be derived using the dynamic version of the principle of virtual displacements [5].

$$\int_0^T (\delta U + \delta V - \delta K) dt = 0 \tag{4.24}$$

Here, the virtual strain energy δU, virtual work done by applied forces δV, and the virtual kinetic energy δK are given by

$$\delta U = \int_{-b/2}^{b/2} \int_{-a/2}^{a/2} \{ \int_{-h/2}^{h/2} [\sigma_x(\delta\varepsilon_x^0 + z\delta\varepsilon_x^1) + \sigma_y(\delta\varepsilon_y^0 + z\delta\varepsilon_y^1)$$
$$+\sigma_{xy}(\delta\gamma_{xy}^0 + z\delta\gamma_{xy}^1) + \sigma_{xz}\delta\gamma_{xz}^0 + \sigma_{yz}\delta\gamma_{yz}^0] dz \}\, dxdy, \tag{4.25}$$

$$\delta V = -\int_{-b/2}^{b/2} \int_{-a/2}^{a/2} (q_o \delta w)\, dxdy - \int_{\Gamma_\sigma} \int_{-h/2}^{h/2} [\widehat{\sigma_{nn}}(\delta u_n + z\delta\phi_n)$$
$$+\widehat{\sigma_{ns}}(\delta u_s + z\delta\phi_s) + \widehat{\sigma_{nz}}\delta w]\, dz\, ds, \tag{4.26}$$

$$\delta K = \int_{-b/2}^{b/2} \int_{-a/2}^{a/2} \int_{-h/2}^{h/2} \rho[(u_{,t}^0 + z\phi_{x,t})(\delta u_{,t}^0 + z\delta\phi_{x,t})$$
$$+(v_{,t}^0 + z\phi_{y,t})(\delta v_{,t}^0 + z\delta\phi_{y,t}) + w_{,t}\delta w_{,t}]\, dz\, dxdy, \tag{4.27}$$

where $(\widehat{\sigma_{nn}}, \widehat{\sigma_{ns}}, \widehat{\sigma_{nz}})$ are the specified stress components on the portion Γ_σ (where natural boundary conditions are imposed) of the boundary Γ, $(\delta u_n, \delta u_s)$ are the virtual displacements along the normal and tangential directions, respectively. The virtual displacements are zero on the portion of the boundary where the corresponding actual displacements are specified. For time dependent problems, the admissible virtual displacements must also vanish at time $t = 0$ and $t = T$.

Substituting for δU, δV and δK from Eqs. (4.25–4.27) into the virtual work statement in Eq. (4.24) and integrating through the laminate,

$$\int_0^T \{ \int_{-b/2}^{b/2} \int_{-a/2}^{a/2} [N_x\delta\varepsilon_x^0 + M_x\delta\varepsilon_x^1 + N_y\delta\varepsilon_y^0 + M_y\delta\varepsilon_y^1$$

$$
\begin{aligned}
&+N_{xy}\delta\gamma^0_{xy} + M_{xy}\delta\gamma^1_{xy} + Q_x\delta\gamma^0_{xz} + Q_y\delta\gamma^0_{yz} - q_o\delta w \\
&-I_0(u^0_{,t}\delta u^0_{,t} + v^0_{,t}\delta v^0_{,t} + w_{,t}\delta w_{,t}) \\
&-I_1(\phi_{x,t}\delta u^0_{,t} + \phi_{y,t}\delta v^0_{,t} + \delta\phi_{x,t}u^0_{,t} + \delta\phi_{y,t}v^0_{,t}) \\
&-I_2(\phi_{x,t}\delta\phi_{x,t} + \phi_{y,t}\delta\phi_{y,t})]\,dxdy \\
-\int_{\Gamma_\sigma} &(\widehat{N_{nn}}\delta u_n + \widehat{N_{ns}}\delta u_s + \widehat{M_{nn}}\delta\phi_n + \widehat{M_{ns}}\delta\phi_s + \widehat{Q_n}\delta w)\,ds\}\,dt = 0
\end{aligned}
\tag{4.28}
$$

is obtained, where I_0, I_1 and I_2 are mass moments of inertia defined as

$$
(I_0, I_1, I_2) = \int_{-h/2}^{h/2} \rho\,(1, z, z^2)\,dz = \sum_i \int_{z_i}^{z_{i+1}} (1, z, z^2)\,\rho^{(i)}\,dz, \tag{4.29}
$$

$\rho^{(i)}$ being the material density of the ith layer.

Substituting virtual strains into Eq. (4.28) and integrating by parts to relieve the virtual general displacements $(\delta u^0, \delta v^0, \delta w, \delta\phi_x, \delta\phi_y)$ of any differentiation,

$$
\begin{aligned}
&\int_0^T \{\int_{-b/2}^{b/2}\int_{-a/2}^{a/2} [-(N_{x,x} + N_{xy,y} - I_0u^0_{,tt} - I_1\phi_{x,tt})\delta u^0 \\
&-(N_{xy,x} + N_{y,y} - I_0v^0_{,tt} - I_1\phi_{y,tt})\delta v^0 \\
&-(M_{x,x} + M_{xy,y} - Q_x - I_2\phi_{x,tt} - I_1u^0_{,tt})\delta\phi_x \\
&-(M_{xy,x} + M_{y,y} - Q_y - I_2\phi_{y,tt} - I_1v^0_{,tt})\delta\phi_y \\
&-(Q_{x,x} + Q_{y,y} + (w_{,x}N_x + w_{,y}N_{xy})_{,x} \\
&+(w_{,x}N_{xy} + w_{,y}N_y)_{,y} + q_o - I_0w_{,tt})\delta w]\,dxdy\}dt \\
&+\int_0^T \int_\Gamma [(N_{nn} - \widehat{N_{nn}})\delta u_n + (N_{ns} - \widehat{N_{ns}})\delta u_s + (Q_n - \widehat{Q_n})\delta w \\
&(M_{nn} - \widehat{M_{nn}})\delta\phi_n + (M_{ns} - \widehat{M_{ns}})\delta\phi_s]\,ds\,dt.
\end{aligned}
\tag{4.30}
$$

The Euler-Lagrange equations are obtained by setting the coefficients of δu^0, δv^0, δw, $\delta\phi_x$ and $\delta\phi_y$ to zero separately.

Then the five equations of motion can be written as

$$
R_1 = N_{x,x} + N_{xy,y} - I_0u^0_{,tt} - I_1\phi_{x,tt} = 0, \tag{4.31}
$$

$$
R_2 = N_{xy,x} + N_{y,y} - I_0v^0_{,tt} - I_1\phi_{y,tt} = 0, \tag{4.32}
$$

$$R_3 = Q_{x,x} + Q_{y,y} + (w_{,x}N_x + w_{,y}N_{xy})_{,x}$$
$$+(w_{,x}N_{xy} + w_{,y}N_y)_{,y} + q_o - I_0 w_{,tt} = 0, \quad \textbf{(4.33)}$$

$$R_4 = M_{x,x} + M_{xy,y} - Q_x - I_2\phi_{x,tt} - I_1 u^0_{,tt} = 0, \quad \textbf{(4.34)}$$

$$R_5 = M_{xy,x} + M_{y,y} - Q_y - I_2\phi_{y,tt} - I_1 v^0_{,tt} = 0. \quad \textbf{(4.35)}$$

The natural boundary conditions are obtained by setting the coefficients of δu_n, δu_s, δw, $\delta\phi_n$ and $\delta\phi_s$ on Γ to zero separately.

The equations of motion in terms of displacements can be obtained by making use of constitutive, strain-displacement and curvature-displacement relations (see [5, 23, 31, 71] for further details).

The equations of motion in dimensionless variables are given below.

$$\psi = \frac{a}{b},\ \bar{x} = \frac{2x}{a},\ \bar{y} = \frac{2y}{b},\ \bar{q} = \frac{q_o a^4}{hD_{11}},\ \bar{u} = \frac{au^0}{h^2},\ \bar{v} = \frac{bv^0}{h^2},\ \bar{w} = \frac{w}{h},$$
$$\xi = \frac{a}{h},\ \eta = \frac{b}{h},\ \bar{\phi}_x = \phi_x\frac{a}{2h},\ \bar{\phi}_y = \phi_y\frac{b}{2h},$$
$$\bar{B}_{ij} = \frac{B_{ij}h}{D_{11}},\ \bar{D}_{ij} = \frac{D_{ij}}{D_{11}} \quad (i,j = 1,2,6),$$
$$\bar{A}_{ij} = \frac{A_{ij}h^2}{D_{11}} \quad (i,j = 1,2,6; i,j = 4,5),$$
$$\bar{t} = \frac{t}{t_0} \quad (t_0 = \sqrt{\frac{a^2b^2h\rho^{(1)}}{4D_{11}}}), \bar{I}_0 = \frac{I_0}{\rho^{(1)}h}, \bar{I}_1 = \frac{I_1}{\rho^{(1)}h^2}, \bar{I}_2 = \frac{I_2}{\rho^{(1)}h^3}. \quad \textbf{(4.36)}$$

$$\bar{R}_1(\bar{u},\bar{v},\bar{w}) = \bar{A}_{11}(\bar{u}_{,\bar{x}\bar{x}} + 2\bar{w}_{,\bar{x}}\bar{w}_{,\bar{x}\bar{x}}) + \bar{A}_{12}\psi^2(\bar{v}_{,\bar{x}\bar{y}} + 2\bar{w}_{,\bar{y}}\bar{w}_{,\bar{x}\bar{y}})$$
$$+\bar{A}_{16}\psi(2\bar{u}_{,\bar{x}\bar{y}} + \bar{v}_{,\bar{x}\bar{x}} + 4\bar{w}_{,\bar{x}}\bar{w}_{,\bar{x}\bar{y}} + 2\bar{w}_{,\bar{y}}\bar{w}_{,\bar{x}\bar{x}})$$
$$+\bar{A}_{26}\psi^3(\bar{v}_{,\bar{y}\bar{y}} + 2\bar{w}_{,\bar{y}}\bar{w}_{,\bar{y}\bar{y}}) + \bar{A}_{66}\psi^2(\bar{u}_{,\bar{y}\bar{y}} + \bar{v}_{,\bar{x}\bar{y}} + 2(\bar{w}_{,\bar{y}}\bar{w}_{,\bar{x}\bar{y}} + \bar{w}_{,\bar{x}}\bar{w}_{,\bar{y}\bar{y}}))$$
$$+2\bar{B}_{11}\bar{\phi}_{x,\bar{x}\bar{x}} + 2\bar{B}_{12}\psi^2\bar{\phi}_{y,\bar{x}\bar{y}} + 2\bar{B}_{16}\psi(2\bar{\phi}_{x,\bar{x}\bar{y}} + \bar{\phi}_{y,\bar{x}\bar{x}})$$
$$+2\bar{B}_{26}\psi^3\bar{\phi}_{y,\bar{y}\bar{y}} + 2\bar{B}_{66}\psi^2(\bar{\phi}_{x,\bar{y}\bar{y}} + \bar{\phi}_{y,\bar{x}\bar{y}})$$
$$-\frac{1}{\eta^2}(\bar{I}_0\bar{u}_{,\bar{t}\bar{t}} + 2\bar{I}_1\bar{\phi}_{x,\bar{t}\bar{t}}) = 0 \quad \textbf{(4.37)}$$

$$\bar{R}_2(\bar{u},\bar{v},\bar{w}) = \bar{A}_{22}(\bar{v}_{,\bar{y}\bar{y}} + 2\bar{w}_{,\bar{y}}\bar{w}_{,\bar{y}\bar{y}}) + \frac{\bar{A}_{12}}{\psi^2}(\bar{u}_{,\bar{x}\bar{y}} + 2\bar{w}_{,\bar{x}}\bar{w}_{,\bar{x}\bar{y}})$$

$$+\frac{\bar{A}_{16}}{\psi^3}(\bar{u}_{,\bar{x}\bar{x}} + 2\bar{w}_{,\bar{x}}\bar{w}_{,\bar{x}\bar{x}}) + \frac{\bar{A}_{26}}{\psi}(\bar{u}_{,\bar{y}\bar{y}} + 2\bar{v}_{,\bar{x}\bar{y}} + 4\bar{w}_{,\bar{y}}\bar{w}_{,\bar{x}\bar{y}} + 2\bar{w}_{,\bar{x}}\bar{w}_{,\bar{y}\bar{y}})$$

$$+\frac{\bar{A}_{66}}{\psi^2}(\bar{v}_{,\bar{x}\bar{x}} + \bar{u}_{,\bar{x}\bar{y}} + 2(\bar{w}_{,\bar{y}}\bar{w}_{,\bar{x}\bar{x}} + \bar{w}_{,\bar{x}}\bar{w}_{,\bar{x}\bar{y}}))$$

$$+2\bar{B}_{22}\bar{\phi}_{y,\bar{y}\bar{y}} + \frac{2\bar{B}_{12}}{\psi^2}\bar{\phi}_{x,\bar{x}\bar{y}} + \frac{2\bar{B}_{16}}{\psi^3}\bar{\phi}_{x,\bar{x}\bar{x}}$$

$$+\frac{2\bar{B}_{26}}{\psi}\bar{\phi}_{x,\bar{y}\bar{y}} + \frac{2\bar{B}_{66}}{\psi}(\bar{\phi}_{x,\bar{x}\bar{y}} + \bar{\phi}_{y,\bar{x}\bar{x}})$$

$$-\frac{1}{\xi^2}(\bar{I}_0\bar{v}_{,\bar{t}\bar{t}} + 2\bar{I}_1\bar{\phi}_{y,\bar{t}\bar{t}}) = 0 \qquad \textbf{(4.38)}$$

$$\bar{R}_3(\bar{u},\bar{v},\bar{w}) = \frac{\bar{A}_{11}}{2\psi^2}(\bar{u}_{,\bar{x}}\bar{w}_{,\bar{x}\bar{x}} + \bar{u}_{,\bar{x}\bar{x}}\bar{w}_{,\bar{x}} + 3\bar{w}_{,\bar{x}\bar{x}}\bar{w}^2_{,\bar{x}})$$

$$+\frac{\bar{A}_{12}}{2}(\bar{u}_{,\bar{x}}\bar{w}_{,\bar{y}\bar{y}} + \bar{w}_{,\bar{y}\bar{y}}\bar{w}^2_{,\bar{x}} + \bar{u}_{,\bar{x}\bar{y}}\bar{w}_{,\bar{y}} + \bar{v}_{,\bar{x}\bar{y}}\bar{w}_{,\bar{x}} + 4\bar{w}_{,\bar{x}}\bar{w}_{,\bar{y}}\bar{w}_{,\bar{x}\bar{y}}$$

$$+\bar{v}_{,\bar{y}}\bar{w}_{,\bar{x}\bar{x}} + \bar{w}_{,\bar{x}\bar{x}}\bar{w}^2_{,\bar{y}}) + \frac{\bar{A}_{22}\psi^2}{2}(\bar{v}_{,\bar{y}\bar{y}}\bar{w}_{,\bar{y}} + \bar{v}_{,\bar{y}}\bar{w}_{,\bar{y}\bar{y}} + 3\bar{w}_{,\bar{y}\bar{y}}\bar{w}^2_{,\bar{y}})$$

$$+\frac{\bar{A}_{16}}{\psi}(\bar{u}_{,\bar{x}\bar{y}}\bar{w}_{,\bar{x}} + \bar{u}_{,\bar{x}}\bar{w}_{,\bar{x}\bar{y}} + 3\bar{w}_{,\bar{x}}(\bar{w}_{,\bar{x}}\bar{w}_{,\bar{x}\bar{y}} + \bar{w}_{,\bar{y}}\bar{w}_{,\bar{x}\bar{x}})$$

$$+\frac{1}{2}(\bar{w}_{,\bar{y}}\bar{u}_{,\bar{x}\bar{x}} + \bar{v}_{,\bar{x}\bar{x}}\bar{w}_{,\bar{x}} + \bar{u}_{,\bar{y}}\bar{w}_{,\bar{x}\bar{x}} + \bar{v}_{,\bar{x}}\bar{w}_{,\bar{x}\bar{x}}))$$

$$+\bar{A}_{26}\psi(\bar{v}_{,\bar{x}\bar{y}}\bar{w}_{,\bar{y}} + \bar{v}_{,\bar{y}}\bar{w}_{,\bar{x}\bar{y}} + 3\bar{w}_{,\bar{y}}(\bar{w}_{,\bar{x}}\bar{w}_{,\bar{y}\bar{y}} + \bar{w}_{,\bar{y}}\bar{w}_{,\bar{x}\bar{y}})$$

$$+\frac{1}{2}(\bar{u}_{,\bar{y}\bar{y}}\bar{w}_{,\bar{y}} + \bar{u}_{,\bar{y}}\bar{w}_{,\bar{y}\bar{y}} + \bar{v}_{,\bar{x}}\bar{w}_{,\bar{y}\bar{y}} + \bar{v}_{,\bar{y}\bar{y}}\bar{w}_{,\bar{x}}))$$

$$+\bar{A}_{66}(\frac{1}{2}\bar{u}_{,\bar{y}\bar{y}}\bar{w}_{,\bar{x}} + \bar{w}_{,\bar{y}\bar{y}}\bar{w}^2_{,\bar{x}} + \frac{1}{2}\bar{u}_{,\bar{x}\bar{y}}\bar{w}_{,\bar{y}} + \frac{1}{2}\bar{v}_{,\bar{x}\bar{y}}\bar{w}_{,\bar{x}}$$

$$+\bar{u}_{,\bar{y}}\bar{w}_{,\bar{x}\bar{y}} + \bar{v}_{,\bar{x}}\bar{w}_{,\bar{x}\bar{y}} + 4\bar{w}_{,\bar{y}}\bar{w}_{,\bar{x}}\bar{w}_{,\bar{x}\bar{y}} + \frac{1}{2}\bar{v}_{,\bar{x}\bar{x}}\bar{w}_{,\bar{y}} + \bar{w}_{,\bar{x}\bar{x}}\bar{w}^2_{,\bar{y}})$$

$$+\bar{A}_{44}\frac{K\xi^2}{4}(\bar{\phi}_{y,\bar{y}} + \bar{w}_{,\bar{y}\bar{y}}) + \bar{A}_{45}\frac{K\xi\eta}{4}(\bar{\phi}_{x,\bar{y}} + \bar{\phi}_{y,\bar{x}} + 2\bar{w}_{,\bar{x}\bar{y}})$$

$$+\bar{A}_{55}\frac{K\eta^2}{4}(\bar{\phi}_{x,\bar{x}} + \bar{w}_{,\bar{x}\bar{x}}) + \frac{\bar{B}_{11}}{\psi^2}(\bar{\phi}_{x,\bar{x}}\bar{w}_{,\bar{x}\bar{x}} + \bar{\phi}_{x,\bar{x}\bar{x}}\bar{w}_{,\bar{x}})$$

$$+\bar{B}_{12}(\bar{\phi}_{x,\bar{x}}\bar{w}_{,\bar{y}\bar{y}} + \bar{\phi}_{x,\bar{x}\bar{y}}\bar{w}_{,\bar{y}} + \bar{\phi}_{x,\bar{x}\bar{y}}\bar{w}_{,\bar{x}} + \bar{\phi}_{y,\bar{y}}\bar{w}_{,\bar{x}\bar{x}})$$

$$+\bar{B}_{22}\psi^2(\bar{\phi}_{,\bar{y}}\bar{w}_{,\bar{y}\bar{y}}+\bar{\phi}_{,\bar{y}\bar{y}}\bar{w}_{,\bar{y}})+\frac{\bar{B}_{16}}{\psi}(2\bar{\phi}_{,\bar{x}}\bar{w}_{,\bar{x}\bar{y}}+2\bar{\phi}_{,\bar{x}\bar{y}}\bar{w}_{,\bar{x}}$$

$$+\bar{\phi}_{,\bar{y}}\bar{w}_{,\bar{x}\bar{x}}+\bar{\phi}_{,\bar{x}}\bar{w}_{,\bar{x}\bar{x}}+\bar{\phi}_{,\bar{x}\bar{x}}\bar{w}_{,\bar{y}}+\bar{\phi}_{,\bar{x}\bar{x}}\bar{w}_{,\bar{x}})$$

$$+\bar{B}_{26}\psi(\bar{\phi}_{,\bar{y}}\bar{w}_{,\bar{y}\bar{y}}+\bar{\phi}_{,\bar{y}\bar{y}}\bar{w}_{,\bar{y}}+\bar{\phi}_{,\bar{y}\bar{y}}\bar{w}_{,\bar{x}}+\bar{\phi}_{,\bar{x}}\bar{w}_{,\bar{y}\bar{y}}+2\bar{\phi}_{,\bar{y}}\bar{w}_{,\bar{x}\bar{y}}+2\bar{\phi}_{,\bar{x}\bar{y}}\bar{w}_{,\bar{y}})$$

$$+\bar{B}_{66}(\bar{\phi}_{,\bar{x}\bar{y}\bar{y}}\bar{w}_{,\bar{x}}+2\bar{\phi}_{,\bar{x}\bar{y}}\bar{w}_{,\bar{x}\bar{y}}+2\bar{\phi}_{,\bar{y}\bar{x}}\bar{w}_{,\bar{x}\bar{y}}+\bar{\phi}_{,\bar{x}\bar{x}\bar{y}}\bar{w}_{,\bar{y}}+\bar{\phi}_{,\bar{y}\bar{x}\bar{y}}\bar{w}_{,\bar{x}}+\bar{\phi}_{,\bar{y}\bar{x}\bar{x}}\bar{w}_{,\bar{y}})$$

$$+\frac{\bar{q}}{16\psi^2}-\frac{\bar{I}_0}{4}\bar{w}_{,\overline{tt}}=0 \tag{4.39}$$

$$\bar{R}_4(\bar{u},\bar{v},\bar{w})=-\bar{A}_{45}\frac{K\psi\xi^2}{2}(\bar{\phi}_{\bar{y}}+\bar{w}_{,\bar{y}})-\bar{A}_{55}\frac{K\xi^2}{2}(\bar{\phi}_{\bar{x}}+\bar{w}_{,\bar{x}})$$

$$+\bar{B}_{11}(\bar{u}_{,\bar{x}\bar{x}}+2\bar{w}_{,\bar{x}}\bar{w}_{,\bar{x}\bar{x}})+\bar{B}_{12}\psi^2(\bar{v}_{,\bar{x}\bar{y}}+2\bar{w}_{,\bar{y}}\bar{w}_{,\bar{x}\bar{y}})$$

$$+\bar{B}_{16}\psi(2\bar{u}_{,\bar{x}\bar{y}}+\bar{v}_{,\bar{x}\bar{x}}+4\bar{w}_{,\bar{x}}\bar{w}_{,\bar{x}\bar{y}}+2\bar{w}_{,\bar{y}}\bar{w}_{,\bar{x}\bar{x}})+\bar{B}_{26}\psi^3(\bar{v}_{,\bar{y}\bar{y}}+2\bar{w}_{,\bar{y}}\bar{w}_{,\bar{y}\bar{y}})$$

$$+\bar{B}_{66}\psi^2(\bar{u}_{,\bar{y}\bar{y}}+\bar{v}_{,\bar{x}\bar{y}}+2\bar{w}_{,\bar{x}}\bar{w}_{,\bar{y}\bar{y}}+2\bar{w}_{,\bar{y}}\bar{w}_{,\bar{x}\bar{y}})$$

$$+2\bar{D}_{11}\bar{\phi}_{,\bar{x}\bar{x}}+2\bar{D}_{12}\psi^2\bar{\phi}_{,\bar{x}\bar{y}}+2\bar{D}_{16}\psi(2\bar{\phi}_{,\bar{x}\bar{y}}+\bar{\phi}_{,\bar{x}\bar{x}})$$

$$+2\bar{D}_{26}\psi^3\bar{\phi}_{,\bar{y}\bar{y}}+2\bar{D}_{66}\psi^2(\bar{\phi}_{,\bar{x}\bar{y}\bar{y}}+\bar{\phi}_{,\bar{y}\bar{x}\bar{y}})-\frac{\bar{I}_1}{\eta^2}\bar{u}_{,\overline{tt}}-\frac{2\bar{I}_2}{\eta^2}\bar{\phi}_{,\overline{tt}}=0 \tag{4.40}$$

$$\bar{R}_5(\bar{u},\bar{v},\bar{w})=-\bar{A}_{44}\frac{K\eta^2}{2}(\bar{\phi}_{\bar{y}}+\bar{w}_{,\bar{y}})-\bar{A}_{45}\frac{K\eta^2}{2\psi}(\bar{\phi}_{\bar{x}}+\bar{w}_{,\bar{x}})$$

$$+\bar{B}_{22}(\bar{v}_{,\bar{y}\bar{y}}+2\bar{w}_{,\bar{y}}\bar{w}_{,\bar{y}\bar{y}})+\frac{\bar{B}_{12}}{\psi^2}(\bar{u}_{,\bar{x}\bar{y}}+2\bar{w}_{,\bar{x}}\bar{w}_{,\bar{x}\bar{y}})$$

$$+\frac{\bar{B}_{16}}{\psi^3}(\bar{u}_{,\bar{x}\bar{x}}+2\bar{w}_{,\bar{x}}\bar{w}_{,\bar{x}\bar{x}})+\frac{\bar{B}_{26}}{\psi}(\bar{u}_{,\bar{y}\bar{y}}+2\bar{v}_{,\bar{x}\bar{y}}+2\bar{w}_{,\bar{x}}\bar{w}_{,\bar{y}\bar{y}}+4\bar{w}_{,\bar{y}}\bar{w}_{,\bar{x}\bar{y}})$$

$$+\frac{\bar{B}_{66}}{\psi^2}(\bar{u}_{,\bar{x}\bar{y}}+\bar{v}_{,\bar{x}\bar{x}}+2\bar{w}_{,\bar{x}}\bar{w}_{,\bar{x}\bar{y}}+2\bar{w}_{,\bar{y}}\bar{w}_{,\bar{x}\bar{x}})$$

$$+2\bar{D}_{22}\bar{\phi}_{,\bar{y}\bar{y}\bar{y}}+\frac{2\bar{D}_{12}}{\psi^2}\bar{\phi}_{,\bar{x}\bar{y}}+\frac{2\bar{D}_{16}}{\psi^3}\bar{\phi}_{,\bar{x}\bar{x}}$$

$$+\frac{2\bar{D}_{26}}{\psi}(\bar{\phi}_{,\bar{y}\bar{y}}+2\bar{\phi}_{,\bar{x}\bar{y}})+\frac{2\bar{D}_{66}}{\psi^2}(\bar{\phi}_{,\bar{x}\bar{y}}+\bar{\phi}_{,\bar{y}\bar{x}})-\frac{\bar{I}_1}{\xi^2}\bar{v}_{,\overline{tt}}-\frac{2\bar{I}_2}{\xi^2}\bar{\phi}_{,\overline{tt}}=0 \tag{4.41}$$

$$\bar{N}_x=\bar{A}_{11}(\bar{u}_{,\bar{x}}+\bar{w}^2_{,\bar{x}})+\bar{A}_{12}\psi^2(\bar{v}_{,\bar{y}}+\bar{w}^2_{,\bar{y}})+\bar{A}_{16}\psi(\bar{u}_{,\bar{y}}+\bar{v}_{,\bar{x}}+2\bar{w}_{,\bar{x}}\bar{w}_{,\bar{y}})$$

$$+2(\bar{B}_{11}\bar{\phi}_{,\bar{x}}+\bar{B}_{12}\psi^2\bar{\phi}_{,\bar{y}}+\bar{B}_{16}\psi(\bar{\phi}_{,\bar{y}}+\bar{\phi}_{,\bar{x}})) \tag{4.42}$$

$$\bar{N}^u_{xy} = \bar{A}_{66}\psi^2(\bar{u}_{,\bar{y}} + \bar{v}_{,\bar{x}} + 2\bar{w}_{,\bar{x}}\bar{w}_{,\bar{y}}) + \bar{A}_{16}\psi(\bar{u}_{,\bar{x}} + \bar{w}^2_{,\bar{x}})$$
$$+\bar{A}_{26}\psi^3(\bar{v}_{,\bar{y}} + \bar{w}^2_{,\bar{y}}) + 2\psi(\bar{B}_{16}\bar{\phi}_{x,\bar{x}} + \bar{B}_{26}\psi^2\bar{\phi}_{y,\bar{y}} + \bar{B}_{66}\psi(\bar{\phi}_{x,\bar{y}} + \bar{\phi}_{y,\bar{x}})) \quad \textbf{(4.43)}$$

$$\bar{N}_y = \bar{A}_{22}(\bar{v}_{,\bar{y}} + \bar{w}^2_{,\bar{y}}) + \frac{\bar{A}_{12}}{\psi^2}(\bar{u}_{,\bar{x}} + \bar{w}^2_{,\bar{x}}) + \frac{\bar{A}_{26}}{\psi}(\bar{u}_{,\bar{y}} + \bar{v}_{,\bar{x}} + 2\bar{w}_{,\bar{x}}\bar{w}_{,\bar{y}})$$
$$+2(\bar{B}_{22}\bar{\phi}_{y,\bar{y}} + \frac{\bar{B}_{12}}{\psi^2}\bar{\phi}_{x,\bar{x}} + \frac{\bar{B}_{26}}{\psi}(\bar{\phi}_{x,\bar{y}} + \bar{\phi}_{y,\bar{x}})) \quad \textbf{(4.44)}$$

$$\bar{N}^v_{xy} = \frac{\bar{A}_{66}}{\psi^2}(\bar{u}_{,\bar{y}} + \bar{v}_{,\bar{x}} + 2\bar{w}_{,\bar{x}}\bar{w}_{,\bar{y}}) + \frac{\bar{A}_{16}}{\psi^3}(\bar{u}_{,\bar{x}} + \bar{w}^2_{,\bar{x}})$$
$$+\frac{\bar{A}_{26}}{\psi}(\bar{v}_{,\bar{y}} + \bar{w}^2_{,\bar{y}}) + 2(\frac{\bar{B}_{16}}{\psi^3}\bar{\phi}_{x,\bar{x}} + \frac{\bar{B}_{26}}{\psi}\bar{\phi}_{y,\bar{y}} + \frac{\bar{B}_{66}}{\psi^2}(\bar{\phi}_{x,\bar{y}} + \bar{\phi}_{y,\bar{x}})) \quad \textbf{(4.45)}$$

$$\bar{M}_x = \bar{D}_{11}\bar{\phi}_{x,\bar{x}} + \bar{D}_{12}\psi^2\bar{\phi}_{y,\bar{y}} + \bar{D}_{16}\psi(\bar{\phi}_{x,\bar{y}} + \bar{\phi}_{y,\bar{x}}) + \frac{\bar{B}_{11}}{2}(\bar{u}_{,\bar{x}} + \bar{w}^2_{,\bar{x}})$$
$$+\frac{\bar{B}_{12}\psi^2}{2}(\bar{v}_{,\bar{y}} + \bar{w}^2_{,\bar{y}}) + \frac{\bar{B}_{16}\psi}{2}(\bar{u}_{,\bar{y}} + \bar{v}_{,\bar{x}} + 2\bar{w}_{,\bar{x}}\bar{w}_{,\bar{y}}) \quad \textbf{(4.46)}$$

$$\bar{M}_y = \bar{D}_{22}\bar{\phi}_{y,\bar{y}} + \frac{\bar{D}_{12}}{\psi^2}\bar{\phi}_{x,\bar{x}} + \frac{\bar{D}_{26}}{\psi}(\bar{\phi}_{x,\bar{y}} + \bar{\phi}_{y,\bar{x}}) + \frac{\bar{B}_{22}}{2}(\bar{v}_{,\bar{y}} + \bar{w}^2_{,\bar{y}})$$
$$+\frac{\bar{B}_{12}}{2\psi^2}(\bar{u}_{,\bar{x}} + \bar{w}^2_{,\bar{x}}) + \frac{\bar{B}_{26}}{2\psi}(\bar{u}_{,\bar{y}} + \bar{v}_{,\bar{x}} + 2\bar{w}_{,\bar{x}}\bar{w}_{,\bar{y}}) \quad \textbf{(4.47)}$$

4.2 Solution Procedure

In the application of the Galerkin method the geometrical boundary conditions are satisfied by choosing appropriate trial functions. For the Galerkin approach, the displacements of the plate are approximated in the form shown below:

$$\bar{u} = \sum_{m=0}^{M}\sum_{n=0}^{N} a_{mn}(\bar{t})U_{mn}(\bar{x},\bar{y}), \quad \textbf{(4.48)}$$

$$\bar{v} = \sum_{m=0}^{M}\sum_{n=0}^{N} b_{mn}(\bar{t})V_{mn}(\bar{x},\bar{y}), \quad \textbf{(4.49)}$$

$$\bar{w} = \sum_{m=0}^{M} \sum_{n=0}^{N} c_{mn}(\bar{t}) W_{mn}(\bar{x}, \bar{y}), \tag{4.50}$$

$$\bar{\phi}_x = \sum_{m=0}^{M} \sum_{n=0}^{N} d_{mn}(\bar{t}) S_{mn}(\bar{x}, \bar{y}), \tag{4.51}$$

$$\bar{\phi}_y = \sum_{m=0}^{M} \sum_{n=0}^{N} e_{mn}(\bar{t}) T_{mn}(\bar{x}, \bar{y}), \tag{4.52}$$

where a_{mn}, b_{mn}, c_{mn}, d_{mn} and e_{mn} are unknown constants, U_{mn}, V_{mn}, W_{mn}, S_{mn} and T_{mn} are the trial functions, and M and N are the number of terms in $\bar{x}$ and $\bar{y}$ directions respectively. Herein, polynomials are used as trial functions, which are chosen to satisfy the geometric boundary conditions, where as natural boundary conditions are not satisfied. In this case, simultaneous approximation is made to the solutions of differential equations and to the boundary conditions.

Trial functions are weighted polynomials given as follows:

$$\begin{aligned} U_{mn} &= \Phi_1 \bar{x}^m \bar{y}^n, \\ V_{mn} &= \Phi_2 \bar{x}^m \bar{y}^n, \\ W_{mn} &= \Phi_3 \bar{x}^m \bar{y}^n, \\ S_{mn} &= \Phi_4 \bar{x}^m \bar{y}^n, \\ T_{mn} &= \Phi_5 \bar{x}^m \bar{y}^n, \end{aligned} \tag{4.53}$$

where Φ_i (i=1, ... 5) denote the weight functions. Substituting Eqs. (4.48–4.52) into nonlinear plate equilibrium equations and the boundary terms yields the residuals in the domain of the plate and at the boundaries of the plate. Forcing these residuals to be orthogonal to each member of a set of trial functions yields the Galerkin equations (4.54–4.58). These equations are solved by employing the Newton-Raphson methodology.

$$\int_{-1}^{+1}\int_{-1}^{+1} U_{mn} \bar{R}_1 d\bar{x} d\bar{y} - \int_{-1}^{+1} U_{mn} \bar{N}_x|_{\bar{x}=\pm 1} d\bar{y} - \int_{-1}^{+1} U_{mn} \bar{N}^u_{xy}|_{\bar{y}=\pm 1} d\bar{x} = 0, \tag{4.54}$$

$$\int_{-1}^{+1}\int_{-1}^{+1} V_{mn} \bar{R}_2 d\bar{x} d\bar{y} - \int_{-1}^{+1} V_{mn} \bar{N}_y|_{\bar{y}=\pm 1} d\bar{x} - \int_{-1}^{+1} V_{mn} \bar{N}^v_{xy}|_{\bar{x}=\pm 1} d\bar{y} = 0, \tag{4.55}$$

$$\int_{-1}^{+1}\int_{-1}^{+1} W_{mn} \bar{R}_3 d\bar{x} d\bar{y} = 0, \tag{4.56}$$

$$\int_{-1}^{+1}\int_{-1}^{+1} S_{mn}\bar{R}_4 d\bar{x}d\bar{y} - \int_{-1}^{+1} S_{mn}\bar{M}_x|_{\bar{x}=\pm 1} d\bar{y} = 0, \tag{4.57}$$

$$\int_{-1}^{+1}\int_{-1}^{+1} T_{mn}\bar{R}_5 d\bar{x}d\bar{y} - \int_{-1}^{+1} T_{mn}\bar{M}_y|_{\bar{y}=\pm 1} d\bar{x} = 0. \tag{4.58}$$

4.3 Boundary Conditions

Six different boundary conditions are considered and shown in Table 4.1. Note that whole plate models are analyzed in all cases presented here. The boundary conditions are

CC–1 : all edges clamped immovable,
CC–2 : clamped, free in the normal and the tangential directions,
CS–1 : simply supported immovable at $x = a/2$ and $y = \pm b/2$,
clamped immovable at $x = -a/2$,
CS–2 : clamped immovable at $x = \pm a/2$ and
simply supported immovable at $y = \pm b/2$,
SS–1 : all edges simply supported immovable,
SS–2 : simply supported, immovable in the normal direction.

Table 4.1: Boundary conditions and corresponding weight functions.

SS–1	$\bar{u} = \bar{v} = \bar{w} = \bar{M}_x = \bar{\phi}_y = 0$ at $\bar{x} = \pm 1$, $\bar{u} = \bar{v} = \bar{w} = \bar{M}_y = \bar{\phi}_x = 0$ at $\bar{y} = \pm 1$. $\Phi_i = (\bar{x}^2 - 1)(\bar{y}^2 - 1)$ $(i = 1, \dots 3)$, $\Phi_4 = (\bar{y}^2 - 1)$, $\Phi_5 = (\bar{x}^2 - 1)$.
SS–2	$\bar{u} = \bar{w} = \bar{M}_x = \bar{\phi}_y = 0$ at $\bar{x} = \pm 1$, $\bar{v} = \bar{w} = \bar{M}_y = \bar{\phi}_x = 0$ at $\bar{y} = \pm 1$. $\Phi_3 = (\bar{x}^2 - 1)(\bar{y}^2 - 1)$, $\Phi_i = (\bar{y}^2 - 1)$ $(i = 2, 4)$, $\Phi_i = (\bar{x}^2 - 1)$ $(i = 1, 5)$.
CC–1	$\bar{u} = \bar{v} = \bar{w} = \bar{\phi}_x = \bar{\phi}_y = 0$ at $\bar{x} = \pm 1$, $\bar{u} = \bar{v} = \bar{w} = \bar{\phi}_x = \bar{\phi}_y = 0$ at $\bar{y} = \pm 1$. $\Phi_i = (\bar{x}^2 - 1)(\bar{y}^2 - 1)$ $(i = 1, \dots 5)$.
CC–2	$\bar{N}_x = \bar{N}^v_{xy} = \bar{w} = \bar{\phi}_x = \bar{\phi}_y = 0$ at $\bar{x} = \pm 1$, $\bar{N}_y = \bar{N}^u_{xy} = \bar{w} = \bar{\phi}_x = \bar{\phi}_y = 0$ at $\bar{y} = \pm 1$. $\Phi_i = 1$ $(i = 1, 2)$, $\Phi_i = (\bar{x}^2 - 1)(\bar{y}^2 - 1)$ $(i = 3, \dots 5)$.
CS–1	$\bar{u} = \bar{v} = \bar{w} = 0$ at $\bar{x} = \pm 1$ and $\bar{y} = \pm 1$, $\bar{\phi}_x = 0$ at $\bar{x} = -1$ and $\bar{y} = \pm 1$, $\bar{M}_x = 0$ at $\bar{x} = 1$, $\bar{M}_y = 0$ at $\bar{y} = \pm 1$, $\bar{\phi}_y = 0$ at $\bar{x} = \pm 1$. $\Phi_i = (\bar{x}^2 - 1)(\bar{y}^2 - 1)$ $(i = 1, \dots 3)$, $\Phi_4 = (\bar{x} + 1)(\bar{y}^2 - 1)$, $\Phi_5 = (\bar{x}^2 - 1)$.
CS–2	$\bar{u} = \bar{v} = \bar{w} = \bar{\phi}_x = 0$ at $\bar{x} = \pm 1$ and $\bar{y} = \pm 1$, $\bar{M}_y = 0$ at $\bar{y} = \pm 1$, $\bar{\phi}_y = 0$ at $\bar{x} = \pm 1$. $\Phi_i = (\bar{x}^2 - 1)(\bar{y}^2 - 1)$ $(i = 1, \dots 4)$, $\Phi_5 = (\bar{x}^2 - 1)$.

5. LARGE DEFLECTION ANALYSIS OF MODERATELY THICK LAMINATED COMPOSITE PLATES

Geometrically nonlinear static response of laminates is investigated using the GM with Newton-Raphson method. FSDT is utilized and strains are chosen in the von Kármán sense.

5.1 Numerical Examples

Large deflection analyses of a symmetric cross-ply laminate and unsymmetric cross-ply and angle-ply laminates are chosen as numerical examples. Note that for all of the analyses the shear correction coefficient $K = 5/6$. The convergence study of the proposed solution technique is carried out and it has been determined that taking M and N as five is appropriate. Hence, for all the GM applications given here, M and N are taken as five.

5.1.1 Symmetric cross-ply laminate

The large deflection of a symmetric cross-ply $[0°/90°/90°/0°]$ laminate under various boundary conditions is analyzed. The Galerkin technique is employed and FSDT is utilized in the formulation of the problem. For the trial function representations $M = N = 5$ in the GM. For this laminate the material properties for each orthotropic lamina and the geometric constants are taken from [23] and given as follows:

$$\begin{aligned} &E_1 = 175.78\,GPa, E_2 = E_1/25, \\ &G_{12}/E_2 = G_{13}/E_2 = 0.5, G_{23}/E_2 = 0.2, \\ &\nu_{12} = 0.25, a = b, a/h = 10. \end{aligned} \tag{5.1}$$

Normalized center deflection and center moment values of the plate under CS–1 and CS–2 boundary conditions for the present technique GM and Chebyshev polynomials applied by Shukla and Nath [23] are given in Figs. (5.1, 5.2). A very close agreement is observed between the GM and CP techniques.

The dimensionless variables presented are

$$q' = \frac{q_o a^4}{E_2 h^4}, w' = \frac{w}{h}, M'_x = \frac{M_x a^2}{D_{11} h}, M'_y = \frac{M_y a^2}{D_{22} h}. \tag{5.2}$$

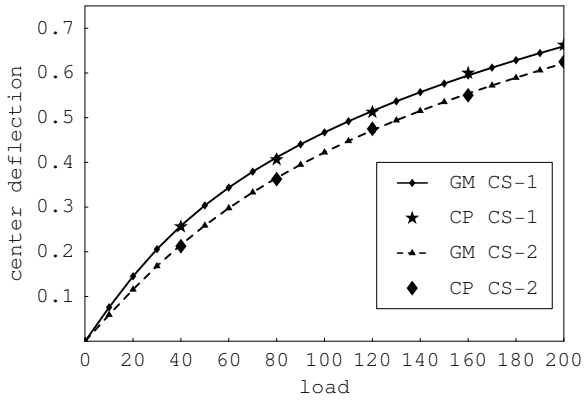


Figure 5.1: Load (q') versus central deflection (w') of [0°/90°/90°/0°] laminate.

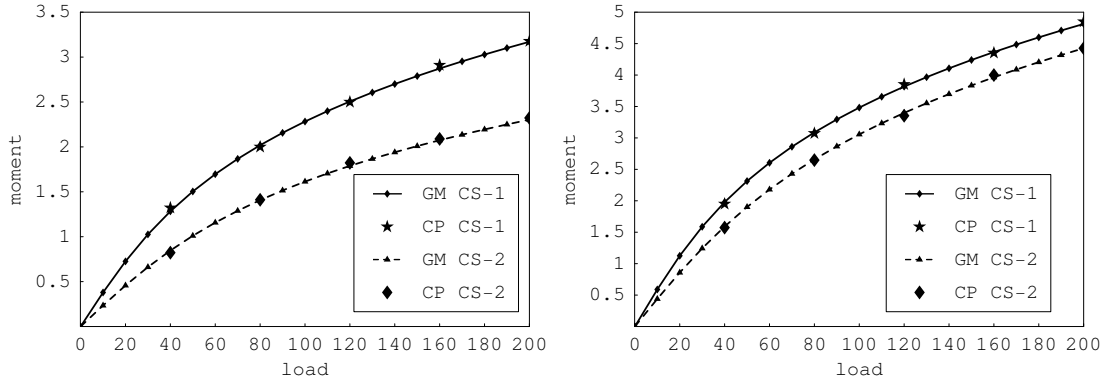


Figure 5.2: Load (q') versus M'_x (a) and M'_y (b) at the center of [0°/90°/90°/0°] laminate.

Table 5.1: Normalized center deflection (w') of the plate under SS–1 boundary condition.

	Load (q')					
a/h	10	20	50	100	150	200
5	0.16195	0.25713	0.41171	0.55262	0.64755	0.72172
10	0.09899	0.18271	0.35054	0.50983	0.61469	0.69501
20	0.07581	0.14581	0.30765	0.47643	0.58935	0.67562
50	0.06868	0.13338	0.29017	0.46121	0.57731	0.66626
CLPT	0.06729	0.13089	0.28640	0.45764	0.57424	0.66363

Table 5.2: Normalized center deflection (w') of the plate under CC–1 boundary condition.

	Load (q')					
a/h	50	100	200	500	750	1000
5	0.36923	0.51802	0.69407	0.98447	1.14032	1.26330
10	0.21535	0.37365	0.57915	0.90767	1.07647	1.20717
20	0.11580	0.22449	0.40896	0.76797	0.95916	1.10566
50	0.07926	0.15672	0.30101	0.63291	0.82677	0.97828
CLPT	0.07160	0.14196	0.27506	0.59400	0.78649	0.93854

The effect of thickness in the FSDT is also investigated using the GM and the related results are shown in Tables (5.1, 5.2). Here, classical laminated plate theory results are obtained employing the GM (see [15] for details).

5.1.2 Unsymmetric laminates

Unsymmetric angle-ply $[45°/-45°]$ and cross-ply $[0°/90°]$ laminates under CC–2 boundary condition are considered for the large deflection analysis. Material and geometrical properties for both cross-ply and angle-ply laminates are taken from [18] and given below.

$$\begin{aligned} &E_2 = E_1/40, G_{12}/E_2 = 0.6, \\ &G_{13}/E_2 = 0.5, G_{23} = G_{13}, \\ &\nu_{12} = 0.25, a = b, a/h = 40, K = 5/6. \end{aligned} \tag{5.3}$$

Dimensionless center deflection and stress versus load curves of these laminates are shown in Figs. 5.3 and 5.4. Here the normalized variables are

$$q' = \frac{q_o a^4}{E_2 h^4} 10^{-2}, w' = \frac{w}{h}, \sigma'_x = \frac{\sigma_x\big|_{\bar{x}=\bar{y}=0}}{E_2}(\frac{a}{h})^2. \tag{5.4}$$

The commercial FEM code ANSYS [72] results for these laminates are found to be in good agreement with the present results (see Figs. 5.3 and 5.4). The stress calculation is carried out at the center of the cross-ply laminate where $z = h/2$ and the results of GM and ANSYS are given in Fig. 5.4. Shell-91 type elements including shear deformations with a 10×10 mesh are used in the ANSYS program.

A convergence study is presented in Figs. 5.5 and 5.6 for the deflection and stress values of the cross-ply laminate at the point of maximum load value, where the

results for different values of M and N are shown. In Fig. 5.6, center deflection and stress versus only the half of the plate coordinate is plotted due to the symmetry. It is observed that the convergence in the case of center deflection is better, as compared to central stress. Note that, the computational cost for $M, N > 9$ is such high that a standard PC configuration at hand is not able to handle the problem.

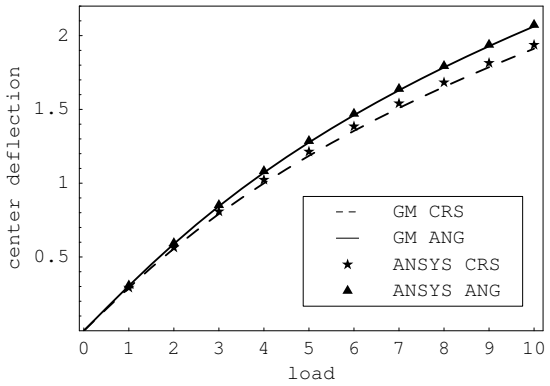


Figure 5.3: Load (q') versus central deflection (w') of cross-ply [0°/90°] (CRS) and angle-ply [45°/ − 45°] (ANG) laminates.

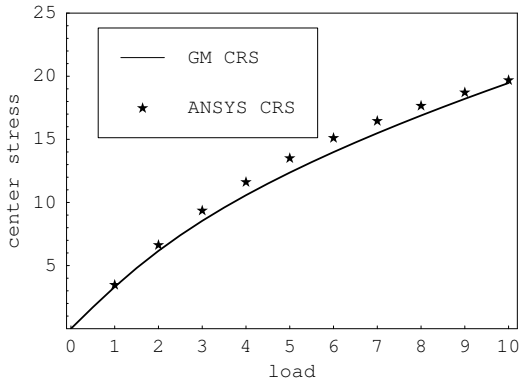
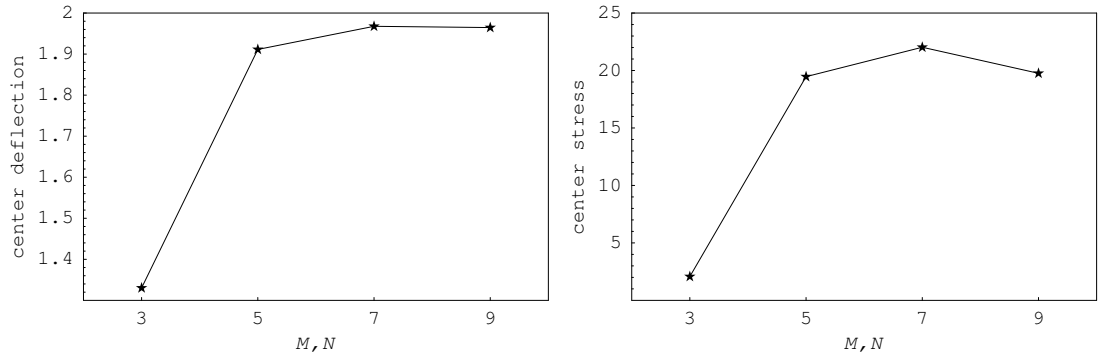
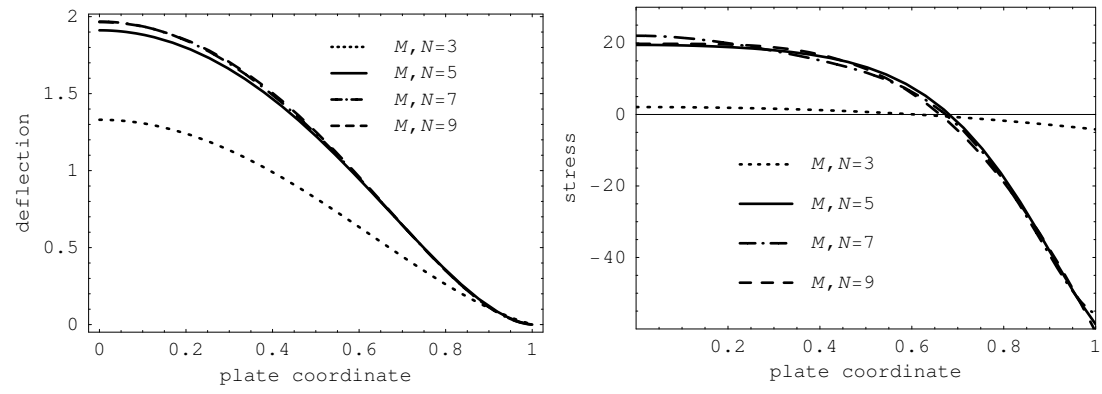


Figure 5.4: Load q' versus center stress $\sigma'_x = \sigma_x|_{\bar{x}=\bar{y}=0}(a/h)^2/E_2$ for cross-ply [0°/90°] (CRS) laminate.



(a) (b)

Figure 5.5: Convergence study for cross-ply laminate (a) center deflection w' (b) center stress σ'_x.



(a) (b)

Figure 5.6: Distribution of (a) center deflection $w'|_{\bar{y}=0}$ and (b) center stress $\sigma'_x|_{\bar{y}=0}$ along the dimensionless plate coordinate $\bar{x}$.

6. NONLINEAR TRANSIENT ANALYSIS

Nonlinear transient analyses of composite plates are performed by using the GM with Newton-Raphson method. Newmark direct time integration technique is employed for time discretization. FSDT and von Kármán type nonlinearity are considered for the present analyses.

6.1 Time Integration

Time integration plays an important role in the linear and nonlinear analyses. The characteristic of the time integration procedure have a critical impact on the feasibility of the calculation. Time integration continues to be an active area of research in numerical analysis.

In many structural dynamics applications only low mode response is of interest. For these cases, the use of unconditionally stable implicit algorithms is generally preferred over conditionally stable algorithms [73]. An integration method is unconditionally stable if the solution for any initial conditions does not grow without bound for any time step. The method is conditionally stable if the above only holds provided that the time step is smaller than a certain value, usually called the stability limit [74]. Conditionally stable algorithms require the size of the time step employed in the temporal discretization process to be inversely proportional to the highest frequency of the discrete system. In practice this is a severe limitation. For this reason, unconditionally stable algorithms are generally preferred.

To integrate Eqs. (4.54–4.58), Newmark's direct integration scheme [75] is employed. In the Newmark scheme the first time derivative of the displacement field $\dot{\mathbf{U}}$ and the solution $\mathbf{U}$ are approximated at $(n+1)$ time step (i.e., at time $t = t_{n+1} \equiv (n+1)\Delta t$) by the following expressions:

$$\dot{\mathbf{U}}_{n+1} = \dot{\mathbf{U}}_n + \Delta t[(1-\gamma)\ddot{\mathbf{U}}_n + \gamma\ddot{\mathbf{U}}_{n+1}], \tag{6.1}$$

$$\mathbf{U}_{n+1} = \mathbf{U}_n + \dot{\mathbf{U}}_n\Delta t + \frac{\Delta t^2}{2}[(1-2\beta)\ddot{\mathbf{U}}_n + 2\beta\ddot{\mathbf{U}}_{n+1}], \tag{6.2}$$

where γ and β parameters are chosen as 1/2 and 1/4 respectively in all of the present analyses. This choice is proposed by Newmark and is known as constant-average-acceleration method that gives an unconditionally stable scheme for linear problems [75].

The selection of the time step can be guided by the following estimate of the time step for conditionally stable time integration schemes:

$$\Delta t^2 \leq \frac{a^2 \left[\rho(1-\nu^2)/E\right]}{2+(1-\nu)\frac{\pi}{12}[1+\frac{3}{2}(\frac{a}{h})^2]} \tag{6.3}$$

Estimate in Eq. (6.3) is given by Tsui and Tong [76] for moderately thick plate theory (see also [77]). Since this estimate is given for an isotropic plate (for linear analyses), it has to be modified according to composite plate properties. Taking the elasticity modulus E_1 of the stiffest lamina and the lowest density ρ among the laminae will be conservative for the stability criteria.

Initial displacement and velocity fields are taken as zero in the analyses. Initial acceleration is obtained by substituting initial displacement field into Eqs. (4.54–4.58) and solving the yielding linear equation system. In each time step, equations of motion is utilized with Newmark's scheme by substituting acceleration at t_{n+1} from Eqs. (4.31–4.35) into the second equation of Newmark scheme. GM is applied to the resulting nonlinear differential equations in terms of displacements at t_{n+1}. The method gives nonlinear equations in terms of unknown coefficients a_{mn}, b_{mn}, c_{mn}, d_{mn} and e_{mn}. These equations are solved by employing the Newton-Raphson methodology. Note that the evaluations of integrals are symbolically computed by using a commercial computer math code $Mathematica^{TM}$ [35].

6.2 Numerical Examples

First, a linear transient analysis of an isotropic square plate is carried out. Then, geometrically nonlinear transient analyses of a symmetric cross-ply laminate and unsymmetric cross-ply and angle-ply laminates are chosen as numerical examples. Note that for all of the analyses the shear correction coefficient $K = 5/6$. As mentioned before, the convergence study of the proposed solution technique is carried out for the static response, and it has been determined that taking M and N as five is appropriate. Also for all the GM applications to transient analyses given here, M and N are taken as five.

6.2.1 Linear transient analysis

Linear transient analysis of an isotropic square plate is chosen for verification case of the present technique. Material, geometric and loading data of the problem are taken from [26] and given below.

$E_2 = 2.1 \times 10^6\, N/cm^2, \rho = 8 \times 10^{-6}\, Nsec^2/cm^4,$

$\nu = 0.25, a = b = 25\, cm, h = 5\, cm, q_o = 10\, N/cm^2.$

The plate is under SS–2 boundary condition. A time step of $2\,\mu sec$ is chosen in the analysis. The center deflection of the present linear analysis are compared with the FEM solutions of Reddy [26] in Fig. 6.1. In the FEM analysis Reddy used 3×3 mesh of shear deformable elements and $\Delta t = 2\,\mu sec$ for the Newmark time integration scheme.

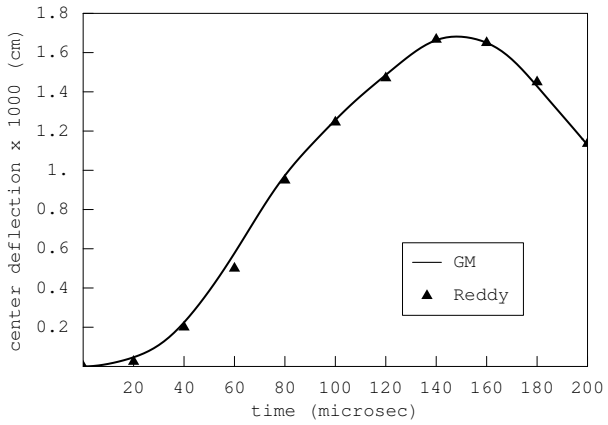


Figure 6.1: Isotropic square plate subjected to uniform pulse loading.

6.2.2 Nonlinear transient analysis of an unsymmetric cross-ply laminate

Nonlinear transient analysis of an unsymmetric cross-ply [0°/90°/0°/90°] laminate is considered. Material, geometric and loading data are taken from [31] and given below.

$E_1/E_2 = 25, G_{12}/E_2 = G_{13}/E_2 = 0.5, G_{23}/E_2 = 0.2,$

$\nu_{12} = 0.25, a = b, a/h = 10.$

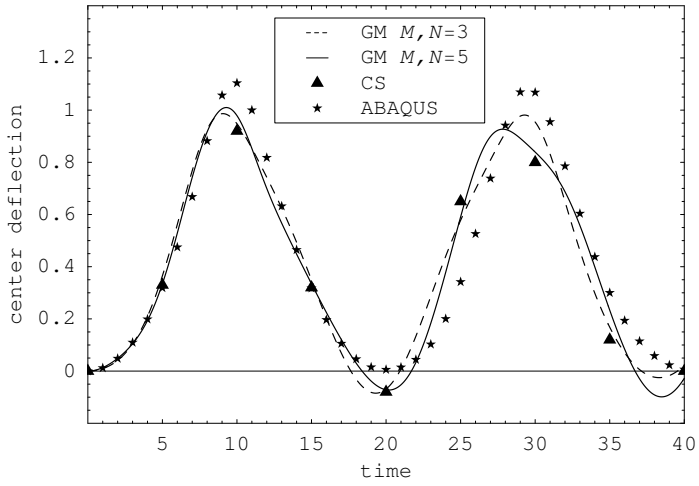


Figure 6.2: Center deflection w' of the cross-ply laminate in time τ.

The dimensionless variables presented are taken as below.

$$q' = \frac{q_o a^4}{E_2 h^4}, w' = \frac{w}{h}, \tau = t\sqrt{\frac{4A_{22}}{I_0 h^2 \xi^2}}. \tag{6.4}$$

The cross-ply laminate is under SS–1 boundary condition and subjected to uniform pulse load $q' = 125$. Results of the present technique GM, CS technique applied by Shukla and Nath [31] and commercial FEM program ABAQUS [78] are given in Fig. 6.2. Here, the time step $\Delta\tau$ is taken as 0.1 in the present technique and ABAQUS analysis. In the ABAQUS analysis 10×10 mesh with S4 type elements is used.

6.2.3 Nonlinear transient analysis of an unsymmetric angle-ply laminate

Nonlinear transient analysis of an angle-ply $[45°/-45°]$ laminate is performed. The material, geometric and loading data are taken from [27] and given below.

$$\begin{aligned} &E_1/E_2 = 25, G_{12}/E_2 = G_{13}/E_2 = 0.5, G_{23}/E_2 = 0.2, \\ &\nu_{12} = 0.25, a = b = 243.8\,cm, h = 0.635\,cm, \\ &\rho = 2.547 \times 10^{-6}\,Nsec^2/cm^4, q_o = 50 \times 10^{-4}\,N/cm^2. \end{aligned} \tag{6.5}$$

The angle-ply laminate is under SS–2 type boundary condition and suddenly applied uniform loading. Here, the time step Δt is taken as $1\,msec$. The center deflection versus time obtained from the present analysis, FEM analysis of Reddy

[27] and ABAQUS analysis is shown in Fig. 6.3. In the ABAQUS analysis 10×10 mesh with S4 type elements and $1\,msec$ as the time step in the Newmark's scheme are used.

Note that the difference of the results from [27] and the others comes from the quarter plate modelling in [27] that is not an actual representation of the full plate model.

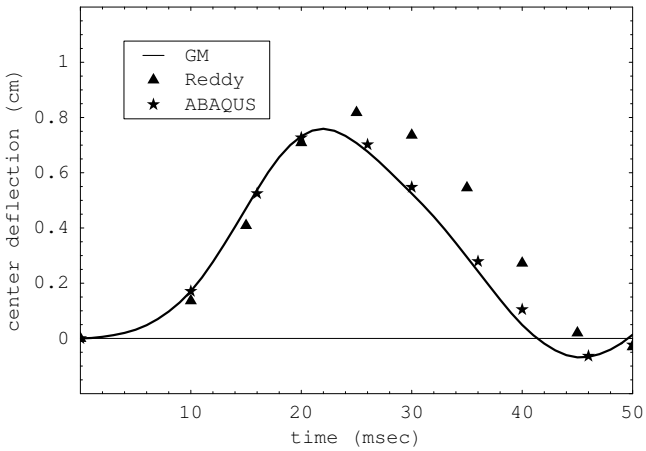


Figure 6.3: Center deflection of the angle-ply laminate in time.

7. CONCLUSIONS AND FUTURE WORK

Large deflection analyses of symmetric and unsymmetric laminates under various boundary conditions are performed by using the Galerkin method with Newton-Raphson technique. The effect of thickness in the FSDT formulation is also investigated. The results are compared to known other approximating methods; Chebyshev polynomials and commercial FEM code ANSYS. A very good agreement is observed. The convergence of the Galerkin method is found to be quite fast for the central displacements but not so fast for the central stresses as it is expected to be. The dynamic large deflection response of composite plates is analyzed by using Galerkin approach with the use of Newmark's scheme in association with Newton-Raphson method. Comparisons with the other techniques such as finite elements, Chebyshev series, and commercial FEM code ABAQUS are given. The method is found to determine closely the displacements with a few number of terms.

The present solution methodology may be used to solve the geometrically nonlinear behavior of the laminates in an easy and effective way with the help of a symbolic math package. The solution process presented here is accomplished in symbolic form and can be adopted to various similar problems. However, the limitations on computing power determine the degree of the approximation.

The first order shear deformation theory is employed for investigation of the shear effects and rotatory inertia. There are other laminate theories mentioned before that can be used for a more detailed analysis on laminates. Application of the present technique to these theories is a future work. In this study only the geometric nonlinearity is considered, material nonlinearity seems to be an other future work for the author. The application of Galerkin method can be extended to analyses, such as post-buckling and large-amplitude vibrations. An estimate on time step for the nonlinear transient analyses is not available in the literature. Time integration procedures can be worked on as a special topic. Also, material damping can easily be treated in the transient analyses already performed.

REFERENCES

[1] **Jones, R.M.**, 1998. Mechanics of Composite Materials, Taylor & Francis Inc., Ann Arbor, MI.

[2] **Hitchings, D.**, 1992. A Finite Element Dynamics Primer, NAFEMS, Glasgow.

[3] **Chia, C.Y.**, 1988. Geometrically non-linear behaviour of composite plates, *ASME Appl. Mech. Rev.*, **41** (12), 439–451.

[4] **Sathyamoorthy, M.**, 1998. Nonlinear Analysis of Structures, CRC Press, New York.

[5] **Reddy, J.N.**, 1997. Mechanics of Laminated Composite Plates, CRC Press, New York.

[6] **Zienkiewicz, O.C. and Morgan, K.**, 1983. Finite Elements and Approximation, John Wiley & Sons, Singapore.

[7] **Finlayson, B.A.**, 1972. The Method of Weighted Residuals and Variational Principles, Academic Press, New York.

[8] **Ray, A.K., Banerjee, B. and Bhattacharjee, B.**, 1992. Large deflections of rhombic plates—a new approach, *Int. J. Non-Linear Mechanics*, **27** (6), 1007–1014.

[9] **Woo, J. and Nair, S.**, 1992. Nonlinear vibrations of rectangular laminated thin plates, *AIAA Journal*, **30** (1), 180–188.

[10] **Savithiri, S. and Varadan, T.K.**, 1993. Large deflection analysis of laminated composite plates, *Int. J. Non-Linear Mechanics*, **28** (1), 1–12.

[11] **Liu, R.-H., Xu, J.-C. and Zhai, S.-Z.**, 1997. Large deflection bending of symmetrically laminated rectilinearly orthotropic elliptical plates including transverse shear, *Archive of Applied Mechanics*, **67**, 507–520.

[12] **Dennis, S.T.**, 1997. A Galerkin solution to geometrically nonlinear laminated shallow shell equations, *Computers & Structures*, **63** (5), 859–874.

[13] **Şenocak, E. and Tanrıöver, H.**, 2001. Large deflection analysis of laminated composite plates, *Proceedings of* 6^{th} *Pasific International Conference on Aerospace Science and Technology*, Kaohsiung, Taiwan.

[14] **Dumir, P.C. and Dube, G.P.**, 2001. Geometrically non-linear analysis of a thick annular plate with elastically constrained edge using Galerkin's method, *Journal of Sound and Vibration*, **246** (3), 556–565.

[15] **Tanrıöver, H. and Şenocak, E.**, 2004. Large deflection analysis of unsymmetrically laminated composite plates: analytical-numerical type approach, *Int. J. Non-Linear Mechanics*, **39** (8), 1385-1392.

[16] **Chia, C.Y. and Prabhakara, M.K.**, 1976. Large deflection of unsymmetric cross-ply and angle-ply plates, *Journal Mechanical Engineering Science*, **18** (4), 179–183.

[17] **Pica, A., Wood, R.D. and Hinton, E.**, 1980. Finite element analysis of geometrically nonlinear plate behavior using a Mindlin formulation, *Computers and Structures*, **11**, 203–215.

[18] **Reddy, J.N. and Chao, W.C.**, 1981. Large-deflection and large-amplitude free vibrations of laminated composite-material plates, *Computers and Structures*, **13**, 341–347.

[19] **Turvey, G.J. and Osman, M.Y.**, 1990. Elastic large deflection analysis of isotropic rectangular Mindlin plates, *Int. J. Mech. Sci.*, **32** (4), 315–328.

[20] **Singh, G., Rao, G.V. and Iyengar, N.G.R.**, 1994. Geometrically nonlinear flexural response characteristics of shear deformable unsymmetrically laminated plates, *Computers and Structures*, **53** (1), 69–81.

[21] **Bencharif, N. and Ng, S.F.**, 1994. Linear and nonlinear deflection analysis of thick rectangular plates–II. Numerical applications, *Computers and Structures*, **50** (6), 763–776.

[22] **Shen, H.-S.**, 1999. Nonlinear bending of Reissner-Mindlin plates with free edges under transverse and in-plane loads and resting on elastic foundations, *International Journal of Mechanical Sciences*, **41**, 845–864.

[23] **Shukla, K.K. and Nath, Y.**, 2000. Nonlinear analysis of moderately thick laminated rectangular plates, *Journal of Engineering Mechanics*, **126** (8), 831–838.

[24] **Liew, K.M., Wang, J., Tan, M.J. and Rajendran, S.**, 2004. Nonlinear analysis of laminated composite plates using the mesh-free kp-Ritz method based on FSDT, *Computer Methods in Applied Mechanics and Engineering*, **193**, 4763–4779.

[25] **Bauer, H.F.**, 1968. Nonlinear response of elastic plates to pulse excitations, *J. Appl. Mech.*, **35** (1), 47–52.

[26] **Reddy, J.N.**, 1983. Dynamic (transient) analysis of layered anisotropic composite-material plates, *Int. J. Num. Meth. Eng.*, **19**, 237–255.

[27] **Reddy, J.N.**, 1983. Geometrically nonlinear transient analysis of laminated composite plates, *AIAA J.*, **21** (4), 621–629.

[28] **Ali, S.A. and Al-Noury, S.**, 1986. Nonlinear dynamic response of rectangular plates, *Computers and Structures*, **22** (3), 433–437.

[29] **Chen, J., Dawe, D.J. and Wang, S.**, 2000. Nonlinear transient analysis of rectangular composite laminated plates, *Composite Structures*, **49**, 129–139.

[30] **Wang, Y.Y., Lam, K.Y. and Liu, G.R.**, 2000. The effect of rotatory inertia on the dynamic response of laminated composite plate, *Composite Structures*, **48**, 265–273.

[31] **Nath, Y. and Shukla, K.K.**, 2001. Non-linear transient analysis of moderately thick laminated composite plates, *Journal of Sound and Vibration*, **247** (3), 509–526.

[32] **Kirby, R.M. and Yosibash, Z.**, 2004. Solution of von Kármán dynamic non-linear plate equations using a pseudo-spectral method, *Computer Methods in Applied Mechanics and Engineering*, **193**, 575–599.

[33] **Sathyamoorthy, M.**, 1987. Nonlinear vibration analysis of plates: A review and survey of current developments, *ASME Appl. Mech. Rev.*, **40** (11), 1553–1561.

[34] **Liew, K.M., Xiang, Y. and Kitipornchai, S.**, 1995. Research on thick plate vibration: A literature survey, *Journal of Sound and Vibration*, **180** (1), 163–176.

[35] **Wolfram, S.**, 1988. *Mathematica*^{TM}: A System for Doing Mathematics by Computer, Addison-Wesley, Redwood City, CA.

[36] **Tanrıöver, H. and Şenocak, E.**, 2004. Dynamic nonlinear behavior of composite plates, *Proceedings of ASCE Aerospace Division International Conference on Engineering, Construction, and Operations in Challenging Environments* (*Earth & Space 2004*), TX, U.S.A., March 07-10.

[37] **Tanrıöver, H. and Şenocak, E.**, Nonlinear transient analysis of orthotropic plates, *Journal of Aerospace Engineering*, submitted.

[38] **Fung, Y.C.**, 1965. Foundations of Solid Mechanics, Prentice-Hall, New Jersey.

[39] **Oden, J.T.**, 1967. Mechanics of Elastic Structures, McGraw-Hill, New York.

[40] **Brush, D.O. and Almroth, B.O.**, 1975. Buckling of Bars, Plates and Shells, McGraw-Hill.

[41] **Novozhilov, V.V.**, 1953. Foundations of The Nonlinear Theory of Elasticity, Graylock Press, Rochester, N.Y.

[42] **Reissner, E.**, 1985. Reflections on the theory of elastic plates, *Appl. Mech. Rev.*, **38** (11), 1453–1464.

[43] **Jemielita, G.**, 1990. On kinematical assumptions of refined theories of plates: A Survey, *J. Appl. Mech.*, **57** (December), 1088–1091.

[44] **Goldenveizer, A.L., Kaplunov, J.D. and Nolde, E.V.**, 1993. On Timoshenko-Reissner type theories of plates and shells, *Int. J. Solids and Structures*, **30** (5), 675–694.

[45] **Lekhnitskii, S.G.**, 1968. Anisotropic Plates 2nd Edition, Translated from the second Russian edition by Tsai, S.W. and Cheron, T., Gordon and Breach Science Publ.

[46] **Whitney, J.M.**, 1987. Structural Analysis of Laminated Anisotropic Plates, Technomic Publ. Co.

[47] **Ambartsumyan, S.A.**, 1991. Theory of Anisotropic Plates: Strenght, Stability, and Vibrations, Hemisphere Publ. Co.

[48] **Reddy, J.N. and Robbins, D.H.**, 1994. Theories and computational models for composite laminates, *ASME Appl. Mech. Rev.*, **47** (6), 147–169.

[49] **Reissner, E.**, 1945. The effect of transverse shear deformation on the bending of elastic plates, *J. Appl. Mech.*, **12**, 69–77.

[50] **Reissner, E.**, 1947. On bending of elastic plates, *Quart. Appl. Math.*, **5** (1), 55–68.

[51] **Mindlin, R.D.**, 1951. Influence of rotatory inertia and shear on flexural motions of isotropic, elastic plates, *J. Appl. Mech.*, **18** (Mar), 31–38.

[52] **Yang, P.C., Norris, C.H. and Stavsky, Y.**, 1966. Elastic wave propagation in heterogeneous plates, *Int. J. Solids and Structures*, **2**, 665–684.

[53] **Whitney, J.M. and Pagano, N.J.**, 1970. Shear deformation in heterogeneous anisotropic plates, *J. Appl. Mech.*, **37** (4), 1031–1036.

[54] **Knight, N.F., and Qi, Y.**, 1997. Restatement of first-order shear deformation theory for laminated plates, *Int. J. Solids and Structures*, **34** (4), 481–492.

[55] **Knight, N.F., and Qi, Y.**, 1997. On a consistent first-order shear deformation theory for laminated plates, *Composites Part B*, **28B**, 397–405.

[56] **Auricchio, F. and Sacco, E.**, 2003. Refined first-order shear deformation theory models for composite laminates, *J. Appl. Mech.*, **70** (May), 381–390.

[57] **Noor, A.K. and Burton, W.S.**, 1989. Assesment of shear deformation theories for multilayered composite plates, *Appl. Mech. Rev.*, **42** (1), 1–13.

[58] **Kapania, R.K. and Raciti, S.**, 1989. Recent advances in analysis of laminated beams and Plates, Part I: Shear effects and Buckling, *AIAA Journal*, **27** (7), 923–934.

[59] **Reddy, J.N.**, 1990. A review of refined theories of laminated plates, *Shock and Vibration Digest*, **22** (7), 3–17.

[60] **Mallikarjuna and Kant, T.**, 1993. A critical review and some results of recently developed refined theories of fiber-reinforced laminated composites and sandwiches, *Composite Structures*, **23**, 293–312.

[61] **Lo, K.H., Christensen, R.M. and Wu, E.M.**, 1977. A high-order theory of plate deformation–Part 2: Laminated plates, *J. Appl. Mech.*, **44** (December), 669–676.

[62] **Reddy, J.N.**, 1984. A simple higher-order theory for laminated composite plates, *J. Appl. Mech.*, **51** (December), 745–752.

[63] **Reddy, J.N.**, 1990. A general non-linear third-order theory of plates with moderate thickness, *Int. J. Non-Linear Mechanics*, **25** (6), 677-686.

[64] **Tan, H.-F., Tian, Z.-H. and Du, X.-W.**, 2000. A new geometrical nonlinear laminated theory for large deformation analysis, *Int. J. Solids and Structures*, **37**, 2577–2589.

[65] **Leung, A.Y.T., Niu, J., Lim, C.W. and Song, K.**, 2003. A new unconstrained third-order plate theory for Navier solutions of symmetrically laminated plates, *Computers and Structures*, **81**, 2539–2548.

[66] **Di Sciuva, M.**, 1987. An improved shear deformation theory for moderately thick multilayered anisotropic shells and plates, *J. Appl. Mech.*, **54** (3), 589–596.

[67] **Murakami, H.**, 1986. Laminated composite plate theory with improved in-plane responses, *J. Appl. Mech.*, **53**, 661–666.

[68] **Mau, S.T.**, 1973. A refined laminated plate theory, *J. Appl. Mech.*, **40** (June), 606–607.

[69] **Reddy, J.N.**, 1987. A generalization of two-dimensional theories of laminated composite plates, *Communications in Applied Numerical Methods*, **3**, 173–180.

[70] **Carrera, E.**, 2000. Historical review of zig-zag theories for multilayered plates and shells, *ASME Appl. Mech. Rev.*, **56** (3), 287–308.

[71] **Turvey, G.J.**, 1995. Buckling and Postbuckling of Composite Plates, Chapman & Hall.

[72] **ANSYS Reference Manual**, 1999. ANSYS Inc.

[73] **Subbaraj, K. and Dokainish, M.A.**, 1989. A survey of direct time integration methods in computational structural dynamics-II. Implicit methods, *Computers and Structures*, **32** (6), 1387–1401.

[74] **Bathe, K.-J.**, 1982. Finite Element Procedures in Engineering Analysis, Prentice-Hall Inc., Englewood Cliffs, New Jersey.

[75] **Newmark, N.M.**, 1959. A method of computation for structural dynamics, *ASCE Journal of the Engineering Mechanics Division*, **8**, 67–94.

[76] **Tsui, T.Y. and Tong, P.**, 1971. Stability of transient solution of moderately thick plate by finite difference method, *AIAA Journal*, **9** (10), 2062–2063.

[77] **Reddy, J.N.**, 1982. On the solutions to forced motions of rectangular composite plates, *J. Appl. Mech.*, **49** (June), 403–406.

[78] **ABAQUS User's Examples and Theory Manuel**, 2003. Version 6.4, ABAQUS, Inc.

VITA

Hakan Tanrıöver was born on March 17, 1976 in Uşak. He completed a Bachelor of Science degree in Mechanical Engineering at Istanbul Technical University in 1998. The author continued his graduate studies at the same department, and received a M.Sc. degree in 2000. He is currently employed as a Research Assistant at Mechanical Engineering Department, Istanbul Technical University.